



**HAL**  
open science

## Collateral Unchained: Rehypothecation networks, concentration and systemic effects

Duc Thi Luu, Mauro Napoletano, Paolo Barucca, Stefano Battiston

### ► To cite this version:

Duc Thi Luu, Mauro Napoletano, Paolo Barucca, Stefano Battiston. Collateral Unchained: Rehypothecation networks, concentration and systemic effects. *Journal of Financial Stability*, 2021, 52, pp.100811. 10.1016/j.jfs.2020.100811 . halshs-03046219

**HAL Id: halshs-03046219**

**<https://shs.hal.science/halshs-03046219>**

Submitted on 13 Feb 2023

**HAL** is a multi-disciplinary open access archive for the deposit and dissemination of scientific research documents, whether they are published or not. The documents may come from teaching and research institutions in France or abroad, or from public or private research centers.

L'archive ouverte pluridisciplinaire **HAL**, est destinée au dépôt et à la diffusion de documents scientifiques de niveau recherche, publiés ou non, émanant des établissements d'enseignement et de recherche français ou étrangers, des laboratoires publics ou privés.



Distributed under a Creative Commons Attribution - NonCommercial 4.0 International License

# Collateral Unchained: Rehypothecation networks, concentration and systemic effects

Duc Thi Luu<sup>1,2</sup>, Mauro Napoletano<sup>\*2,3,6</sup>, Paolo Barucca<sup>4,5</sup>, and Stefano Battiston<sup>5</sup>

<sup>1</sup>Department of Economics, University of Kiel, Germany

<sup>2</sup>Sciences Po, OFCE, Paris, France

<sup>3</sup>SKEMA business school, Université Côte dAzur

<sup>4</sup>Department of Computer Science, University College London, London, UK

<sup>5</sup>Department of Banking and Finance, University of Zurich, Switzerland

<sup>6</sup>Institute of Economics, Scuola Superiore SantAnna, Pisa, Italy

February 13, 2020

## Abstract

We study how the practice of collateral rehypothecation impacts the generation of liquidity and the emergence of systemic liquidity risk, and how both depend on the structure of the financial network. We build a basic model where banks interact via chains of “repo” contracts (i.e. repurchasing agreements) and use their proprietary collateral or re-use the collateral obtained by other banks via “reverse repos”. We then extend the model to allow banks to determine endogenously the optimal amount of collateral to rehypothecate, based on the equilibrium level of Value-at-Risk. In this framework, we first show how total collateral volume and its velocity are affected by characteristics of the network such as the length of rehypothecation chains and the existence of closed (i.e. cyclic) chains of contracts, the presence of sink nodes (wherein collateral remains trapped), the direction of collateral flows, and the density of the network. We then demonstrate that a trade-off between liquidity and systemic risk exists for certain classes of networks structures. On the one hand, we show that structures where collateral flows are concentrated among fewer densely connected nodes allow for larger collateral volumes, even at low levels of network density. On the other hand, the same networks are also more exposed to larger cascades of collateral hoarding, as a result of localized liquidity shocks.

Keywords: Rehypothecation, Collateral, Repo Contracts, Networks, Liquidity, Collateral-Hoarding Effects, Systemic Risk. JEL Codes: G01, G11, G32, G33.

---

\*Corresponding author: OFCE-Sciences Po, Department of Innovation and Competition, 60, rue Dostoevski BP 85 - 06902 Sophia Antipolis Cedex, France; E-mail: [mauro.napoletano@sciencespo.fr](mailto:mauro.napoletano@sciencespo.fr)

# 1 Introduction

This paper investigates the dynamics of collateral and its implications in terms of systemic liquidity risk when financial actors are connected in a network of financial contracts and can rehypothecate the collateral. Collateral is of increasing importance for the functioning of the global financial system. One reason is that the non-bank/bank nexus has become considerably more complex over the past two decades. Indeed, the separation between hedge funds, mutual funds, insurance companies, banks, and broker/dealers has become blurred as a result of financial innovation and deregulation (Singh, 2016; Pozsar and Singh, 2011). Another reason for the significant increase in collateral volumes (comparable to M2 until the recent financial crisis, see e.g. Singh, 2011) has been the diffusion of rehypothecation agreements. The role of collateral in lending agreements is to protect the lender against a borrower’s default. Rehypothecation<sup>1</sup> is the right of the lender to re-use the collateral to secure another transaction in the future (see Monnet, 2011).

Rehypothecation of collateral has clear advantages for liquidity in modern financial systems (see Financial Stability Board, 2017b). In particular, it allows parties to increase the availability of assets to secure their loans, since a given pool of collateral can be re-used to support different financial transactions. As a result, rehypothecation increases the funding liquidity of agents (see Brunnermeier and Pedersen, 2008). At the same time, rehypothecation also implies risks for market players. First, one risk associated with the additional funding liquidity allowed by rehypothecation can be the building-up of excessive leverage in the market (see e.g. Bottazzi et al., 2012; Singh, 2012; Capel and Levels, 2014). Second, rehypothecation implies that several agents are counting on the same set of collateral to secure their transactions. It follows that rehypothecation may represent yet another channel through which agents’ balance sheets become interlocked<sup>2</sup>, and thus a source of distress propagation and of systemic risk. For instance in the face of idiosyncratic shocks, some institutions may start to precautionarily hoard collateral, which in turn constrains the availability of collateral and its re-use for the downstream institutions in re-pledging chains. This may lead to an inefficient market freeze if participants lack the necessary assets to secure their loans (Leitner, 2011; Monnet, 2011; Gorton and Metrick, 2012). The latter is the distress channel we focus on in this paper.

To analyze economic benefits and systemic consequences of rehypothecation, we develop a model of collateral dynamics over a network of bilateral<sup>3</sup> repurchase agreements (repos) across

---

<sup>1</sup>Throughout this paper, the terms “re-use”, “rehypothecation”, and “re-pledge” are interchangeable.

<sup>2</sup>See Battiston et al. (2016) for an account of the sources of banks’ interconnectedness in financial systems.

<sup>3</sup>Bilateral repos still account for a sizeable portion of the market in the US and for the largest share in Europe. For the US, the (rough) estimates provided by (Copeland et al., 2014), indicate that for the period from July to August 2008, the market share of tri-party repo activity was 40% whereas the one of bilateral repos was 60%. Furthermore, the work by Keller et al. (2014) finds that bilateral repos between banks account for the largest

financial actors, which we refer to as “banks” hereafter.<sup>4</sup> A “repo” or “repurchase agreement”, is the sale of securities together with an agreement for the seller to buy back the securities at a later date. A “reverse repo” is the same contract from the point of view of the buyer.

To keep the model as simple as possible, we abstract from many features of actual repo markets, like heterogeneous collateral quality, maturity and heterogeneous haircut rates and we assume that the amount of collateral available for secured financing is set as a constant fraction of total collateral available to each agent. The latter includes the proprietary collateral endowment of each bank as well as the collateral obtained from other banks via reverse repos.

Although simple, our model allows us to identify features of the rehypothecation network topology that determine (i) the overall volume of collateral in the market, and (ii) the velocity of collateral (Singh, 2011). We show that both variables are an increasing function of the length of open chains. However, for a given length, cyclic chains (i.e. those where banks are organized in a cycle of repo contracts) produce higher collateral than a-cyclic chains. At the same time, even in networks with similar cyclic chains, the presence of sinks, i.e. nodes where the collateral remains trapped, imply differences on the total amount of collateral. Indeed collateral sinks emerge in our analysis as a crucial notion to understand the relation between network structure and collateral flows.

Furthermore, we show that the direction of collateral flows also matters. In particular, concentrating collateral flows among few nodes organized in a cyclic chain allows larger increases in collateral volume and in velocity even with small chains’ length. Finally, we investigate total collateral under some typical network architectures, which capture different modes of organization of financial relations in markets, and in particular different degrees of heterogeneity in the distribution of repo contracts and of collateral flows. We show that total collateral is an increasing function of the density of financial contracts in the random network (where heterogeneity is mild) and in the core-periphery network (where heterogeneity is high). However, core-periphery structures where collateral flows are concentrated among nodes in the core allow a greater increase in collateral already at low levels of network density.

The model described so far with fixed hoarding rates is useful to analyse the effects of network topology on collateral flows. At the same time, it is unfit to study the systemic risk implications of rehypothecation, since hoarding behaviour could also reflect the liquidity position of the

---

share of the repo market in the European Union.

<sup>4</sup>Our choice to focus on banks at this stage is motivated by empirical evidence that, at least in some countries, a good deal of collateral re-use takes place via security refinancing operations that occurs among banks. This is for instance one of the key results emerging from the study by Keller et al. (2014) based on a sample of 38 EU banks, which are the main players in the management of securities collateral in the European Union market. Similarly, Baranova et al. (2016) stress how every unit of collateral that passes from the primary providers of collateral (typically hedge funds) to cash lenders (typically money market funds) has to pass through a chain of intermediaries (3.9 on average in their study), which are typically credit institutions.

other agents in the network. We thus extend the model in order to capture the fact that banks endogenously determine their level of rehypothecation and hoarding, based on their expectations on liquidity risk. More precisely, we assume that hoarding rates are set according to a Value-at-Risk (VaR) criterion, aimed at minimizing liquidity default risk. In this framework, we show that the equilibrium hoarding rate of each bank is a function of the hoarding rates and the collateral levels of the banks at which it is directly and indirectly connected. This mechanism introduces important collateral hoarding externalities in the dynamics, as an increase in hoarding at some banks may indirectly cause higher hoarding at other banks, even if only indirectly connected to it and far away from it in the network. We then use the extended model to study the impact on total collateral losses of small uncertainty shocks hitting a fraction of banks in the network, and how those losses vary with the structure of the rehypothecation networks.

We show that core-periphery structures are the most exposed to large collateral losses when shocks hit the central nodes in the network, i.e. the one concentrating collateral flows. As, core-periphery are also the structures that generate larger collateral volumes, our results highlight that these structures are characterized by a trade-off between creation of liquidity and systemic liquidity risk.

Our work is related to the growing literature on financial networks that analyses the conditions for systemic risk to emerge and the relation between network structure and the systemic impact of shocks. Within this literature, some works have focused on the shock transmission channel on the asset side, based on a mechanism of default contagion. Many of these works are based on the model of Eisenberg and Noe (2001), that addresses the problem of payment clearing in a network of obligations. Rogers and Veraart (2013) extends the model of Eisenberg and Noe (2001) to allow for the possibility of some loss amplification. However, in their extension, systemic risk can only emerge as a result of many initial defaults in the network. Similarly, the work of Acemoglu et al. (2015), identifies a trade-off on the shock size and shows that in the case of extremely large shocks, a dense network can be more fragile than a sparser one. It should be noticed that the works based on Eisenberg and Noe (2001) do not capture an important feature of the 2008 financial crisis, i.e. the emergence of systemic risk from the combination of small shocks (indeed the subprime mortgage market was small compared to global financial markets) in the presence of mispricing, leverage and interconnectedness (see also Visentin et al., 2016, for a discussion) .

Motivated by the limitations of the default contagion approach, a parallel stream of works has focused on distress contagion, by building on the work by Battiston et al. (2012). This research strand builds on the idea that contagion can occur not just through the propagation of realized losses, but also through expected losses. In this framework, the presence of bankruptcy costs and specific cyclical chains of contracts are sufficient conditions for the instability of the

financial system (Bardoscia et al., 2017), leading to a trade-off in the relation between financial stability and network density, even for a same level of shock size.

Remarkably, the two streams of literature on default contagion and on distress contagion can be reconciled in a unified framework of network asset valuation (Barucca et al., 2017). The impact of the network structure on systemic risk has also been investigated in terms of default probability, by providing conditions on leverage and recovery rate such that more dense networks imply a higher probability of systemic defaults (Battiston et al., 2016). These issues about contagion in financial networks and the challenges ahead for the field of financial stability are summarized in Battiston and Martínez-Jaramillo (2018).

In a nutshell, one key result of the above stream of literature is that the density of financial contracts leads to a trade-off between the benefits of individual risk diversification and the danger of systemic risk. Similarly, our work shows that higher density of collateral rehypothecation linkages leads, in some specific network structures, to a trade-off between the creation of liquidity and the emergence of systemic liquidity risk. However, while the aforementioned literature focuses on contagion in the sense of (expected) losses on asset values, our work focuses on contagion in the sense of liquidity shocks.

More specifically, our work contributes also to the recent theoretical literature on the consequences of collateral rehypothecation (see e.g. Bottazzi et al., 2012; Andolfatto et al., 2017; Gottardi et al., 2017; Singh, 2016). This literature has highlighted the role of rehypothecation in determining repo rates (e.g. Bottazzi et al., 2012), or in softening borrowing constraints of market participants and in shaping the interactions in repo markets (Gottardi et al., 2017; Andolfatto et al., 2017) or, finally, it has contributed to evaluate some welfare aspects of policies aimed at regulating rehypothecation (Andolfatto et al., 2017). However, to the best of our knowledge, our paper is the first to study the role of the structure of the network of collateral exchanges and to explore how different network structures determine overall collateral volumes and velocity. Furthermore, our work contributes also to the literature on liquidity hoarding cascades, where it builds in particular on the work of Gai et al. (2011). However, differently from that work, our model introduces endogenously hoarding rates that depend on the liquidity of the bank and its position in the network. In addition, it shows that the liquidity hoarding dynamics can have different consequences depending on the specific structure of the network.

The paper is organized as follows. Section 2 introduces the basic definitions used throughout the paper and the model with fixed hoarding rates. Section 3 studies in detail how the structure of rehypothecation networks determines collateral volume and its velocity. Next, Section 4 extends the model to feature time-varying hoarding rates determined according to a VaR criterion. Section 5 uses the latter model to study collateral hoarding cascades in different rehypothecation networks. Finally, Section 6 concludes, also by discussing some implications of our work.

## 2 A simple model of collateral dynamics on networks

In this section we build the basic model that we then use to analyse how network structure affects collateral volumes and velocity in presence of rehypothecation. We start with the basic definitions that we shall use throughout the paper. We then introduce the laws governing collateral dynamics in presence of rehypothecation and with banks having exogenous hoarding levels.

### 2.1 Definitions

Consider a set of  $N$  financial institutions (“banks” for brevity in the following). Banks invest into an external asset, that yields an exogenously fixed return  $r_{EA}$ , and that can also be used as a collateral. In, addition they lend to each other by using only secured loans that involve exchange of collateral as in Singh (2011).<sup>5</sup> More precisely, we assume that all debt contracts are “repo” contracts, they are thus secured by collateral. The haircut rate of a repo, that we denote as  $h$ , is a percentage that is subtracted from the market value of an asset that is being used in a repo transaction.<sup>6</sup> To collect funds via repo contracts each bank  $i$  ( $1 \leq i \leq N$ ) can use the collateral that it has in its “box”. The box includes the proprietary collateral or the collateral obtained via reverse-repos, which can then be re-pledged or rehypothecated for further repo transactions.

Repo transactions among banks using proprietary and non-proprietary collateral occur through a directed network  $\mathcal{G}$ , that we shall label “rehypothecation network”. More precisely, the rehypothecation network corresponds to a static network of repo contracts. The proprietary collateral of banks travels through the network and it can be used or re-used in contracts occurring at different time steps across the counter-parties defined by the network. It is useful to define the following notations to characterize the different flows of collateral in each bank’s box:

- $A_i^{C^{out}}$ : the amount of collateral flowing out of the box of bank  $i$ , i.e. the amount of collateral that bank  $i$  uses to obtain loans from other banks.
- $A_i^{C^{rm}}$ : the amount of (re-pledgeable) collateral remaining inside the box.
- $A_i^C$ : the amount of (pledgeable) collateral flowing into the box of bank  $i$ . By construction, we have  $A_i^C = A_i^{C^{out}} + A_i^{C^{rm}}$ . Notice that  $A_i^C$  includes both proprietary as well as non-proprietary assets received from other banks.

---

<sup>5</sup>See also Aguiar et al. (2016) for a more comprehensive discussion of the structure of collateral flows.

<sup>6</sup>The size of the haircut usually reflects the perceived risk associated with holding the asset. In addition, the repurchase price in repos should be greater than the original sale price, the difference effectively representing interest, and sometimes called the repo rate. We do not account for the role played by the repo rate in our model.

- $A_i^0$ : the value of the proprietary collateral of bank  $i$ . This means bank  $i$  is the original owner of  $A_i^0$ .
- $B_i$ : the borrowers' set of bank  $i$ , i.e. the banks that obtained funding from  $i$  via repos and thus provided collateral to  $i$ . In the rehypothecation network,  $B_i$  is also the “in-neighborhood” of  $i$ .
- $L_i$ : the lenders' set of bank  $i$ , i.e. the banks that obtained collateral from  $i$  and thus provided funding to  $i$ . In the rehypothecation network,  $L_i$  is also the ‘out-neighborhood’ of  $i$ .<sup>7</sup>

Furthermore, let the variable  $a_{i \leftarrow j}$  capture the direction of collateral flow from bank  $j$  to bank  $i$ . In particular, for every pair of banks  $i$  and  $j$ ,  $a_{i \leftarrow j} = 1$  if bank  $j$  has given collateral to bank  $i$  and  $a_{i \leftarrow j} = 0$  otherwise. Two additional variables related to direction of collateral flows are the “out-degree” of a bank  $i$ ,  $k_i^{out}$ , which measures the total number of outgoing links of the bank, and thus the number of banks to whom bank  $i$  provided collateral to. Likewise, the “in-degree” of a bank  $i$ ,  $k_i^{in}$ , is the total number of banks that provided collateral to  $i$ .

Finally, we assume that each bank hoards a fraction  $(1 - \theta_i)$  of the collateral it has in the box. More precisely, for every monetary unit of collateral, bank  $i$  keeps  $(1 - \theta_i)$  inside its box and gives away  $\theta_i$ . Moreover, to keep the model simple, we assume that each bank homogeneously spreads its non-hoarded collateral across its lenders. Let  $s_{i \leftarrow j}$  be the share of bank  $j$ 's outgoing collateral flowing into the box of bank  $i$ . If  $L_j = \emptyset$  (i.e.  $k_j^{out} = 0$ ), then all shares  $s_{i \leftarrow j}$  are equal to zero. If the lender's set is not void,  $L_j \neq \emptyset$ , that is if  $k_j^{out} > 0$ , then the total outgoing collateral (pledged or re-pledged) by bank  $j$  is equal to

$$\sum_{i \in L_j} s_{i \leftarrow j} A_j^{Cout} = A_j^{Cout}.$$

Accordingly, the shares  $s_{i \leftarrow j}$  satisfy the constraint  $\sum_{i \in L_j} s_{i \leftarrow j} = 1$ . Notice, that this means that each non-zero column of the matrix of shares  $\mathcal{S} = \{s_{i \leftarrow j}\}_{N \times N}$  associated with the network  $\mathcal{G}$  is summing to 1. In addition, recall that collateral is spread homogeneously across lenders. This implies that the elements of the matrix  $\mathcal{S}$  can be expressed as

$$\begin{cases} s_{i \leftarrow j} = \frac{a_{i \leftarrow j}}{k_j^{out}}, & \text{if } k_j^{out} > 0, \\ s_{i \leftarrow j} = 0, & \text{otherwise.} \end{cases} \quad (1)$$

---

<sup>7</sup>Throughout this paper, lenders stand for those who lend money and receive collateral while in the opposite side, borrowers are those who give collateral and receive cash.

## 2.2 Collateral dynamics

To describe collateral dynamics in our model, let us denote by  $A_{i,t}^{C^{rm}}$  the cumulative (re-pledgeable) collateral flow inside the box up to time step  $t$ , and by  $A_{i,t}^{C^{out}}$  the cumulative flow of collateral that has been going out of the box up to time step  $t$ . The cumulative flow of pledgeable collateral  $A_{i,t}^C$  that bank  $i$  has had up to time step  $t$  is then defined as the sum of the latter two quantities  $A_{i,t}^C = A_{i,t}^{C^{out}} + A_{i,t}^{C^{rm}}$ . Also, throughout the paper, when dropping the time step  $t$ , the notations  $A_i^C$ ,  $A_i^{C^{rm}}$  and  $A_i^{C^{out}}$  will denote the values for  $A_{i,t}^C$ ,  $A_{i,t}^{C^{rm}}$  and  $A_{i,t}^{C^{out}}$  at the equilibrium.

Furthermore, let us assume, in line with Bottazzi et al. (2012), that the amount of collateral that can be rehypothecated never exceeds the amount of collateral net of the haircut. In addition, assume for simplicity that the haircut rate  $h \in [0, 1]$  is the same for all banks. On these grounds, we can write the following expression for the dynamics of  $A_{i,t}^{C^{out}}$  ( $t \geq 2$ ), the cumulative outflow of collateral from the box of bank  $i$  up to time  $t$ :

$$A_{i,t}^{C^{out}} = A_i^{0^{out}} + (1-h)\delta_i\theta_i \sum_{j \in B_i} s_{i \leftarrow j} A_{j,t-1}^{C^{out}}, \quad (2)$$

where  $A_i^{0^{out}} = A_{i,1}^{0^{out}} = \delta_i\theta_i A_i^0$  is the proprietary amount of outgoing collateral of bank  $i$ . The second term of the equation captures the amount of collateral received by  $i$  from its borrowers  $j$  and that is re-pledged. Notice that bank  $i$  can only re-pledge a fraction  $(1-h)\theta_i$  of what it receives, where  $(1-h)$  accounts for the fraction remaining after the haircut is applied, and the parameter  $\theta_i$  accounts for the fraction that is not hoarded. Finally,  $\delta_i$  is an indicator equal to one if bank  $i$  engages in at least one repo contract, so that its out-degree is positive, and equal to zero otherwise (i.e.  $\delta_i = 1$ , if  $k_i^{out} > 0$ , and zero otherwise). In equilibrium, we can re-express equation (2) as follows:

$$A_i^{C^{out}} = A_i^{0^{out}} + (1-h)\delta_i\theta_i \sum_{j \in B_i} s_{i \leftarrow j} A_j^{C^{out}}. \quad (3)$$

Similarly, the dynamics of the cumulative flow of re-pledgeable collateral remaining inside the box of bank  $i$  up to time  $t$  is described by the following equation:

$$A_{i,t}^{C^{rm}} = A_i^{0^{rm}} + (1-h)(1-\delta_i\theta_i) \sum_{j \in B_i} s_{i \leftarrow j} A_{j,t-1}^{C^{out}}, \quad (4)$$

where  $A_i^{0^{rm}} = A_{i,1}^{0^{rm}} = A_i^0 - A_i^{0^{out}} = (1-\delta_i\theta_i)A_i^0$  is the initial remaining collateral.

In equilibrium, equation (4) reads

$$A_i^{C^{rm}} = A_i^{0^{rm}} + (1-h)(1-\delta_i\theta_i) \sum_{j \in B_i} s_{i \leftarrow j} A_j^{C^{out}}. \quad (5)$$

Uses and re-uses of collateral in our model are fully described by the recursive process explained by equations (2) and (4). Specific examples illustrating uses and re-uses of collateral governed by the above equations are provided in Section 3.1 and 3.2. Notice also that these two equations imply that at the beginning of the process every bank  $i$  gives away  $A_i^{0^{out}}$  of collateral to its outgoing neighbors and keeps  $A_i^{0^{rm}}$  inside its box. In addition, for an amount of  $s_{i \leftarrow j} A_{j,t-1}^{C^{out}}$  that bank  $i$  receives from a neighbour  $j$  at step  $t-1$ , it re-pledges  $(1-h)\delta_i\theta_i s_{i \leftarrow j} A_{j,t-1}^{C^{out}}$  and hoards an amount  $[1-(1-h)\delta_i\theta_i] s_{i \leftarrow j} A_{j,t-1}^{C^{out}}$  at time  $t$ . However, only the amount  $(1-h)(1-\delta_i\theta_i) s_{i \leftarrow j} A_{j,t-1}^{C^{out}}$  of this hoarded collateral is further re-pledgeable to obtain further funding later, because the amount of collateral related to the haircut,  $h s_{i \leftarrow j} A_{j,t-1}^{C^{out}}$ , is kept in a segregated account that can be only accessed in the case of a credit event (see Bottazzi et al., 2012, for details).<sup>8</sup>

We can also determine the expression of the cumulative flow of re-pledgeable collateral that bank  $i$  has had up to time  $t$ :

$$A_{i,t}^C = A_{i,t}^{C^{out}} + A_{i,t}^{C^{rm}} = A_i^0 + (1-h) \sum_{j \in B_i} s_{i \leftarrow j} A_{j,t-1}^{C^{out}}. \quad (6)$$

The last equation makes clear that the total pledgeable collateral flow that a bank has had,  $A_{i,t}^C$ , includes the proprietary assets (i.e.  $A_i^0$ ) as well as re-pledgeable non-proprietary assets (i.e.  $(1-h) \sum_{j \in B_i} s_{i \leftarrow j} A_{j,t-1}^{C^{out}}$ ) received from other banks via reverse repos. Notice that  $A_{i,t-1}^{C^{rm}} = (1-\delta_i\theta_i) A_{i,t-1}^C$  and that  $A_{i,t-1}^{C^{out}} = \delta_i\theta_i A_{i,t-1}^C$ . Substituting the latter expression in equation (6) we obtain a system of equations in the variables  $A_{i,t}^C$ :

$$A_{i,t}^C = A_i^0 + (1-h) \sum_{j \in B_i} s_{i \leftarrow j} \delta_j \theta_j A_{j,t-1}^C. \quad (7)$$

Similarly, in the equilibrium equation (7) reads

$$A_i^C = A_i^0 + (1-h) \sum_{j \in B_i} s_{i \leftarrow j} \delta_j \theta_j A_j^C. \quad (8)$$

The possibility of collateral use and re-use changes over time, as inflows and outflows of collateral in a bank's box change over time as a consequence of the different uses and re-uses of collateral made by other banks in the network. In addition, the very possibility of re-using

---

<sup>8</sup>Notice that the segregated amount  $h s_{i \leftarrow j} A_{j,t-1}^{C^{out}} = [1-(1-h)\delta_i\theta_i] s_{i \leftarrow j} A_{j,t-1}^{C^{out}} - (1-h)(1-\delta_i\theta_i) s_{i \leftarrow j} A_{j,t-1}^{C^{out}}$ . In this paper we focus on the re-pledgeable part of collateral.

collateral is clearly constrained by the maturity of a repo contract  $T_{repo}$ . In what follows, we shall assume that the maturity of repo contracts is sufficiently long. Moreover, we shall focus on equilibrium collateral. This equilibrium corresponds to the cumulative collateral flow generated by the system over an infinite amount of steps of collateral uses and re-uses. In particular, we shall focus henceforth only on the equilibrium outflowing collateral,  $A^{C^{out}}$  (equilibrium collateral henceforth). Indeed, first, via equation (6) remaining collateral  $A^{C^{rm}}$  is also determined in equilibrium once the amount of outflowing collateral  $A^{C^{out}}$  and the initial proprietary collateral  $A^0$  are known. Second, outflowing collateral is a very interesting variable in our model, as it captures each bank's contribution to overall collateral flows, and thus to overall funding liquidity in the market.

To find the equilibrium collateral outflow, let us start by writing equation (3) in matrix form

$$A^{C^{out}} = A^{0^{out}} + (1 - h)\mathcal{M}A^{C^{out}} \quad (9)$$

where the elements  $\mathcal{M}$  is the adjacency matrix of the rehypothecation network  $\mathcal{G}$ , with elements  $m_{i \leftarrow j}$  defined as:

$$\begin{cases} m_{i \leftarrow j} = \delta_i \theta_i s_{i \leftarrow j} = \frac{\delta_i \theta_i a_{i \leftarrow j}}{k_j^{out}}, & \text{if } k_j^{out} > 0, \\ m_{i \leftarrow j} = 0, & \text{if } k_j^{out} = 0. \end{cases}$$

Given the network of collateral flows  $\mathcal{G}$ , the haircut rate  $h$ , and the vector of non-hoarded rates  $\theta = \{\theta_i\}_{i=1}^n$ , we obtain  $A^{C^{out}}$  by solving equation (9):

$$A_E^{C^{out}} = (\mathcal{I} - (1 - h)\mathcal{M})^{-1} A^{0^{out}} = \mathcal{B}_1 A^{0^{out}}, \quad (10)$$

with  $\mathcal{I}$  denoting the identity matrix of size  $N$ , and with<sup>9</sup>  $\mathcal{B}_1 = (\mathcal{I} - (1 - h)\mathcal{M})^{-1}$ . The above equation indicates that the equilibrium amount of collateral created will be, in general, a function of the entire topology of the rehypothecation network  $\mathcal{G}$  and of the vector of non-hoarding rates  $\theta = \{\theta_i\}_{i=1}^N$ . In the next sections, we focus on the case of exogenous hoarding rates, and we study the role of the network topology in affecting collateral flows.

### 3 Rehypothecation networks and endogenous borrowing capacity

We shall now describe how the structure of the rehypothecation network affects equilibrium collateral outflow determined according to the model developed in the previous section. To perform our investigation it is useful to define some aggregate indicators measuring the performance of a

---

<sup>9</sup>Note that  $\mathcal{B}_1$  exists if  $0 < h < 1$  and  $0 \leq \theta_i \leq 1$ . A detailed proof is provided in the Appendix.

network in affecting collateral flows. The first one is the aggregate cumulative collateral outflow,  $S^{out}$ , or “total collateral” henceforth, which is defined as:

$$S^{out} = \sum_{i=1}^{i=N} A_i^{C^{out}}. \quad (11)$$

In addition, we also introduce the “collateral multiplier”<sup>10</sup>,  $m$ . It is defined as:

$$m = \frac{\sum_{i=1}^{i=N} A_i^{C^{out}}}{\sum_{i=1}^{i=N} A_i^{0^{out}}} = \frac{S^{out}}{S^{0^{out}}}, \quad (12)$$

where  $S^{0^{out}} = \sum_{i=1}^{i=N} A_i^{0^{out}}$  is the initial aggregate flow of proprietary collateral provided by banks. Throughout the paper, we shall focus on  $S^{out}$  and  $m$  when analyzing collateral flows in a given network  $\mathcal{G}$ . Notice that  $S^{out}$  captures the aggregate flow of collateral provided by banks in the financial system. A higher (lower) amount of this flow indicates a more liquid market, i.e. one where agents can easily find collateral to secure their financial transactions. In addition,  $m$  captures the “velocity” of collateral when rehypothecation is allowed (see also Singh, 2011; Keller et al., 2014).<sup>11</sup> Again, a higher (lower) value of  $m$  indicates a more (less) liquid market, and in particular one where the same set of collateral can secure a larger set of secured lending contracts. In particular, a multiplier higher than one indicates a market where banks can secure more borrowing than what is allowed by the initial proprietary collateral outflow. In that respect, we shall say that a rehypothecation network  $\mathcal{G}$  generates “endogenous borrowing capacity” whenever the collateral multiplier associated with it is larger than one ( $m > 1$ ).<sup>12</sup>

Both performance indicators are affected by the hoarding behavior of banks in the network. To simplify the analysis in this section we shall assume the non-hoarding and hoarding rates are fixed, so that  $\theta_i = \bar{\theta}$  and  $(1 - \theta_i) = (1 - \bar{\theta})$ ,  $\forall i$ . In Section 4, we shall remove this restriction, and we consider that banks can set endogenously these coefficients according to a VaR criterion in presence of liquidity shocks.

We shall begin our analysis by providing stylized examples and by stating propositions that show how the aggregate flow of collateral going out of the boxes of all banks,  $S^{out}$ , and the collateral multiplier,  $m$ , are influenced by some key characteristics of rehypothecation networks,

<sup>10</sup>See Financial Stability Board (2017a) for discussions of other collateral re-use measures.

<sup>11</sup>Our definition of collateral multiplier is based on the ratio between total collateral that banks make available for re-use (both proprietary and received) and the initial proprietary collateral that banks make available for re-use. Notice that our definition of multiplier differs from the one in Singh (2011), that is measured as the ratio between total collateral received and primary sources of collateral, but it is similar to the one introduced by Keller et al. (2014).

<sup>12</sup>Notice that this term should not be confused with the term used to describe the nature of the hoarding rates, which we will refer to as “exogenous” (i.e. fixed) in Sections 3 and as “endogenous” (i.e. dynamically determined by each taking into account counterparties’ choices) in Sections 4 and 5.

like the length of rehypothecation chains, the presence of cyclic chains, or the direction of collateral flows and the presence of collateral “sinks” wherein collateral remains trapped. These results also shed light on the core mechanisms driving the generation of endogenous borrowing capacity and of collateral hoarding cascades in more complex network architectures.

### 3.1 Length of chains and network cycles

Let us start with simple examples of chains composed by three banks as shown in Figure 1: panel (a) a star chain, panel (b) an open chain, and panel (c) a closed chain or a “cycle”.

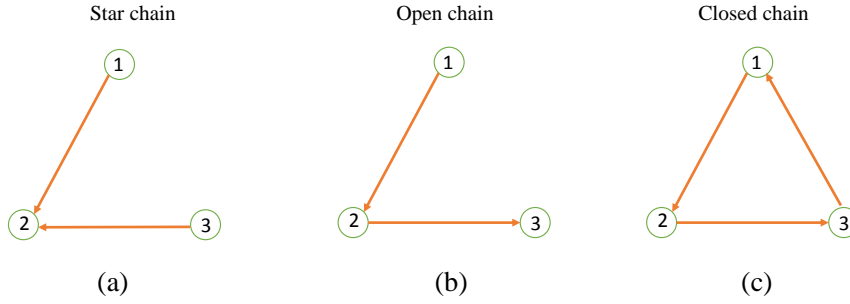


Figure 1: Examples of rehypothecation chains among three banks.

#### *Star chains*

In the first case (i.e. the star chain in Figure 1 (a)), B2 receives collateral from B1 and B3, and then it does not re-use it. In this case there is no endogenous borrowing capacity in the system. Before discussing the example, we denote by  $A_{i,T}^{C^{out}}$  the cumulative collateral outflow from the box of bank  $i$  after  $T$  times. In addition,  $S_{a,T}^{out}$  total collateral after  $T$  times and  $m_{a,T}$  the corresponding collateral multiplier.<sup>13</sup> At  $t = 1$ , the collateral outflows from the boxes of B1, B2, B3 are:

$$\begin{cases} A_{1,t=1}^{C^{out}} = A_1^{0^{out}} = \theta_1 A_1^0 \text{ (going to bank 2)} \\ A_{2,t=1}^{C^{out}} = A_2^{0^{out}} = 0 \\ A_{3,t=1}^{C^{out}} = A_3^{0^{out}} = \theta_3 A_3^0 \text{ (going to bank 2)} \end{cases} \quad (13)$$

<sup>13</sup>Notice that  $A_i^{C^{out}}$  mentioned in equation (10) is equilibrium collateral, and it corresponds to the cumulative collateral outflow when  $T \rightarrow +\infty$ .

At  $t = T \geq 2$ ,  $A_i^{C^{out}}$  remains constant  $\forall i$  since there is no re-use of collateral. We can write

$$\begin{pmatrix} A_{1,t=T}^{C^{out}} \\ A_{2,t=T}^{C^{out}} \\ A_{3,t=T}^{C^{out}} \end{pmatrix} = \begin{pmatrix} A_1^{0^{out}} \\ A_2^{0^{out}} \\ A_3^{0^{out}} \end{pmatrix} + (1-h)M_a \begin{pmatrix} A_1^{0^{out}} \\ A_2^{0^{out}} \\ A_3^{0^{out}} \end{pmatrix}, \quad (14)$$

where

$$M_a = \begin{bmatrix} 0 & 0 & 0 \\ 0 & 0 & 0 \\ 0 & 0 & 0 \end{bmatrix}.$$

It follows that total collateral in the example of Figure 1 (a) is always equal to the sum of the initial proprietary collateral outflow from banks' boxes and thus, that there is no creation of endogenous borrowing capacity. That is, we get:

$$S_a^{out} = S_{a,T}^{out} = \sum_{i=1}^{i=3} A_{i,T}^{C^{out}} = A_1^{0^{out}} + A_3^{0^{out}}, \quad (15)$$

and

$$m_a = m_{a,T} = \frac{\sum_{i=1}^{i=3} A_{i,T}^{C^{out}}}{\sum_{i=1}^{i=3} A_i^{0^{out}}} = 1. \quad (16)$$

### *A-cyclic chains*

We now consider the second example represented by the “open chain” or “a-cyclic chain” in Figure 1 (b). In this case B2 re-uses the collateral that it receives from B1. In presence of rehypothecation the network generates endogenous borrowing capacity,  $S^{0^{out}} > S^0$ . However, this possibility is constrained by the length of the open chain (equal to 2 in the example shown in the figure). At  $t = 1$ , the collateral outflows from the boxes of B1, B2, B3 are:

$$\begin{cases} A_{1,t=1}^{C^{out}} = A_1^{0^{out}} = \theta_1 A_1^0 \text{ (going to bank 2)} \\ A_{2,t=1}^{C^{out}} = A_2^{0^{out}} = \theta_2 A_2^0 \text{ (going to bank 3)} \\ A_{3,t=1}^{C^{out}} = A_3^{0^{out}} = 0 \end{cases} \quad (17)$$

At  $t = 2$ , bank 2 will re-use a fraction  $\theta_2$  of an additional re-pledgeable collateral that it has

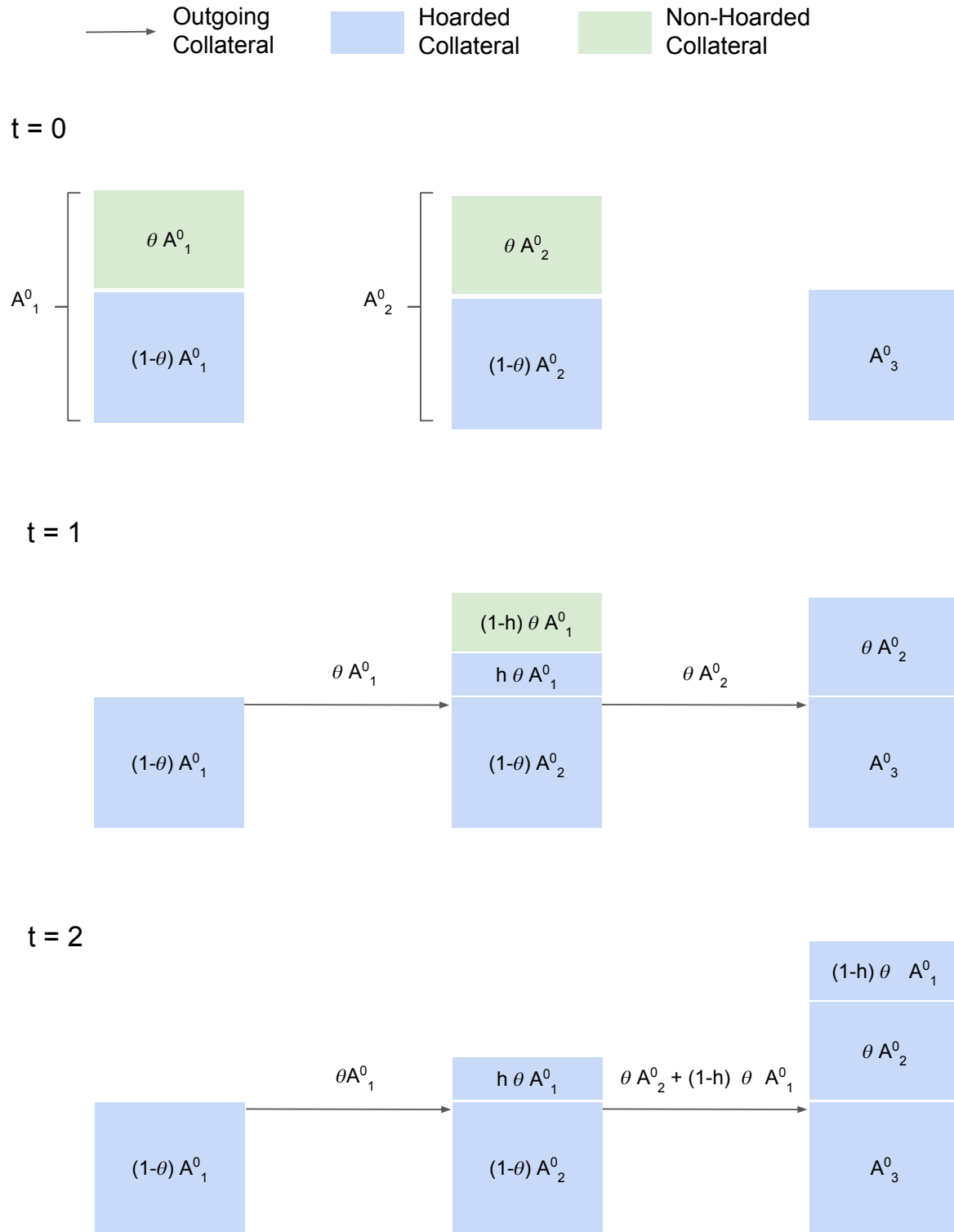


Figure 2: Collateral dynamics in the rehypothecation chain among three banks corresponding to case (b) in Figure 1.

received from bank 1 at time  $t = 1$ . Therefore, cumulative collateral outflows read as:

$$\begin{cases} A_{1,t=2}^{Cout} = A_1^{0out} \\ A_{2,t=2}^{Cout} = A_2^{0out} + (1-h)\theta_2 A_1^{0out} \\ A_{3,t=2}^{Cout} = A_3^{0out} \end{cases} \quad (18)$$

which in matrix form reads

$$\begin{pmatrix} A_{1,t=2}^{Cout} \\ A_{2,t=2}^{Cout} \\ A_{3,t=2}^{Cout} \end{pmatrix} = \begin{pmatrix} A_1^{0out} \\ A_2^{0out} \\ A_3^{0out} \end{pmatrix} + (1-h)M_b \begin{pmatrix} A_1^{0out} \\ A_2^{0out} \\ A_3^{0out} \end{pmatrix}, \quad (19)$$

where now

$$M_b = \begin{bmatrix} 0 & 0 & 0 \\ \theta_2 & 0 & 0 \\ 0 & 0 & 0 \end{bmatrix}.$$

Since all elements of  $M_b^t$  are equal to zero for all  $t \geq 2$ , we get that the equilibrium values of total collateral and of the collateral multiplier are:

$$\begin{pmatrix} A_{1,t=T}^{Cout} \\ A_{2,t=T}^{Cout} \\ A_{3,t=T}^{Cout} \end{pmatrix} = \begin{pmatrix} A_{1,t=2}^{Cout} \\ A_{2,t=2}^{Cout} \\ A_{3,t=2}^{Cout} \end{pmatrix} \quad (\forall T \geq 2).$$

In addition,

$$S_b^{out} = S_{b,T}^{out} = \sum_{i=1}^{i=3} A_{i,t=T}^{Cout} = A_1^{0out} + A_2^{0out} + \theta_2(1-h)A_1^{0out}, \quad (20)$$

and

$$m_b = m_{b,T} = \frac{\sum_{i=1}^{i=3} A_{i,t=T}^{Cout}}{\sum_{i=1}^{i=3} A_i^{0out}} = 1 + \theta_2(1-h) \frac{A_1^{0out}}{A_1^{0out} + A_2^{0out}}. \quad (21)$$

Notice that the above collateral multiplier is larger than 1 as long as  $h < 1$  and  $\theta_2 > 0$ .

Figure 2 illustrates the collateral dynamics unfolding in this simple open chain. In the figure, hoarded collateral is shown in blue and non-hoarded collateral is indicated in green. Furthermore, the values above the arrows indicate the cumulative collateral outflows at each time step. At time  $t = 0$ , no outgoing collateral is present. At time  $t = 1$  some collateral outflows from bank 1 towards bank 2, and the same occurs from bank 2 to bank 3. The hoarded collateral of bank 2 has now increased and bank 2 has additional non-hoarded collateral that can be rehypothecated. At time  $t = 2$ , bank 2 further transfers the non-hoarded collateral possessed at time  $t = 1$  to

bank 3. This transfer implies some collateral re-use, as it includes also the collateral received from bank 1 in the previous time step.

### *Cyclic chains*

We now consider the third case when rehypothecation processes among banks create a closed chain or a “cycle”, like the one in Figure 1 (c). Notice that in the above example every bank has a positive out-degree, i.e.  $k_i^{out} > 0, \forall i = 1, 2, 3$  and accordingly,  $\delta_i = 1, \forall i = 1, 2, 3$  (cf. Section 2.2). We will now show that the creation of endogenous borrowing capacity is no longer constrained by the length of the chain and that total collateral and the multiplier are larger than in previous example.

At  $t=1$ , the collateral outflows are:

$$\begin{cases} A_{1,t=1}^{Cout} = A_1^{0out} = \theta_1 A_1^0 \text{ (going to bank 2)} \\ A_{2,t=1}^{Cout} = A_2^{0out} = \theta_2 A_2^0 \text{ (going to bank 3)} \\ A_{3,t=1}^{Cout} = A_3^{0out} = \theta_3 A_3^0 \text{ (going to bank 1)} \end{cases} \quad (22)$$

Furthermore, at  $t=2$ , each bank  $i$  will re-use a fraction  $\theta_i$  of the additional re-pledgeable collateral that it has received from other banks at the previous time step. We thus get:

$$\begin{cases} A_{1,t=2}^{Cout} = A_1^{0out} + \theta_1(1-h)A_3^{0out} \\ A_{2,t=2}^{Cout} = A_2^{0out} + \theta_2(1-h)A_1^{0out} \\ A_{3,t=2}^{Cout} = A_3^{0out} + \theta_3(1-h)A_2^{0out} \end{cases} \quad (23)$$

and in matrix form,

$$\begin{pmatrix} A_{1,2}^{Cout} \\ A_{2,2}^{Cout} \\ A_{3,2}^{Cout} \end{pmatrix} = \begin{pmatrix} A_1^{0out} \\ A_2^{0out} \\ A_3^{0out} \end{pmatrix} + (1-h)M_c \begin{pmatrix} A_1^{0out} \\ A_2^{0out} \\ A_3^{0out} \end{pmatrix}, \quad (24)$$

where

$$M_c = \begin{bmatrix} 0 & 0 & \theta_1 \\ \theta_2 & 0 & 0 \\ 0 & \theta_3 & 0 \end{bmatrix}.$$

Notice that in (23)  $\theta_1(1-h)A_3^{0out}$ ,  $\theta_2(1-h)A_1^{0out}$ ,  $\theta_3(1-h)A_2^{0out}$  are, respectively, the additional flows of collateral that banks 1, 2, and 3 receive from all other banks. Moreover, at  $t = 3$ , each bank  $i$  will again re-use a fraction  $\theta_i$  of the additional re-pledgeable collateral that it has received

from other banks at time  $t = 2$ . We thus get:

$$\begin{cases} A_{1,t=3}^{Cout} = A_1^{0out} + \theta_1 A_3^{0out} (1-h) + \theta_1 (1-h) \theta_3 (1-h) A_2^{0out} \\ A_{2,t=3}^{Cout} = A_2^{0out} + \theta_2 A_1^{0out} (1-h) + \theta_2 (1-h) \theta_1 (1-h) A_3^{0out} \\ A_{3,t=3}^{Cout} = A_3^{0out} + \theta_3 A_2^{0out} (1-h) + \theta_3 (1-h) \theta_2 (1-h) A_1^{0out} \end{cases} \quad (25)$$

which in matrix form reads,

$$\begin{pmatrix} A_{1,3}^{Cout} \\ A_{2,3}^{Cout} \\ A_{3,3}^{Cout} \end{pmatrix} = \begin{pmatrix} A_1^{0out} \\ A_2^{0out} \\ A_3^{0out} \end{pmatrix} + [(1-h)M_c]^1 \begin{pmatrix} A_1^{0out} \\ A_2^{0out} \\ A_3^{0out} \end{pmatrix} + [(1-h)M_c]^2 \begin{pmatrix} A_1^{0out} \\ A_2^{0out} \\ A_3^{0out} \end{pmatrix} \quad (26)$$

In general, at  $t = T + 1$ , i.e. after  $T$  times of collateral re-uses, the cumulative collateral outflows are:

$$\begin{pmatrix} A_{1,T+1}^{Cout} \\ A_{2,T+1}^{Cout} \\ A_{3,T+1}^{Cout} \end{pmatrix} = \{I + [(1-h)M_c]^1 + [(1-h)M_c]^2 + \dots + [(1-h)M_c]^T\} \begin{pmatrix} A_1^{0out} \\ A_2^{0out} \\ A_3^{0out} \end{pmatrix}. \quad (27)$$

Expressed differently,

$$\begin{pmatrix} A_{1,T+1}^{Cout} \\ A_{2,T+1}^{Cout} \\ A_{3,T+1}^{Cout} \end{pmatrix} = \begin{pmatrix} A_1^{0out} \\ A_2^{0out} \\ A_3^{0out} \end{pmatrix} + (1-h)M_c \begin{pmatrix} A_{1,T}^{Cout} \\ A_{2,T}^{Cout} \\ A_{3,T}^{Cout} \end{pmatrix}. \quad (28)$$

Clearly, the additional flow of collateral in the system is now equal to

$$[[(1-h)M_c]^1 + ((1-h)M_c)^2 + \dots + ((1-h)M_c)^T] \begin{pmatrix} A_1^{0out} \\ A_2^{0out} \\ A_3^{0out} \end{pmatrix}.$$

Finally, when  $T \rightarrow \infty$ , we obtain the equilibrium values for  $S_c^{out}$  and for  $m_c$ . Their expressions are the following:

$$S_c^{out} = \lim_{t \rightarrow \infty} S_{c,t}^{out} = \lim_{t \rightarrow \infty} \sum_{i=1}^{i=3} A_{i,t}^{Cout}, \quad (29)$$

and

$$m_c = \lim_{t \rightarrow \infty} m_{c,t} = \lim_{t \rightarrow \infty} \frac{\sum_{i=1}^{i=3} A_{i,t}^{Cout}}{\sum_{i=1}^{i=3} A_i^{0out}}. \quad (30)$$

To conclude, it is interesting to notice that, as long as  $\{A_i^0\}_{i=1}^{i=3}$  and  $\{\theta_i\}_{i=1}^{i=3}$  are homogeneous

across banks, we have the following ranking  $S_c^{out} > S_b^{out} > S_a^{out}$  and  $m_c > m_b > m_a$ .

### 3.2 Direction of collateral flows, collateral sinks and cycles' length

The above examples have clarified the fundamental properties that a rehypothecation network must have in order to create additional liquidity in the system. In particular, the second example (the a-cyclic chain) makes clear that the possibilities of additional liquidity creation are determined by the length of re-pledging chains among banks. In addition, the third example (the cyclic chain) shows that the presence of cycles is necessary to maximize collateral flows in a network. Furthermore, networks wherein collateral flows all end up in a cycle will, *coeteris paribus*, create more endogenous borrowing capacity than networks where some collateral leaks out from cycles and ends up in *sinks*, i.e. nodes from which it cannot escape. To better clarify the foregoing statement, we consider in Figure 3, three example networks of five nodes with the same number of links. In addition, in these networks, all out-degrees are positive, and consequently collateral from each node will flow into a cycle after going through some directed edges<sup>14</sup>, and there is no leakage from the cycle. The only difference among the three networks is in the length of the cycles. Nevertheless, we will show that as long as non-hoarding rates are constant and homogeneous, the three networks generate in equilibrium the same total collateral and they have the same multiplier. This is summarized in the following proposition.

**Proposition 1.** Let  $\theta_i = \theta$  ( $\forall i$ ). For the networks in panels  $\alpha = a, b, c$  of Figure (3)  $S_{\alpha,t}^{out} = \sum_{i=1}^{i=5} A_{i,t}^{C^{out}}$ ,  $\forall t \geq 1$ .

*Proof.* See appendix. □

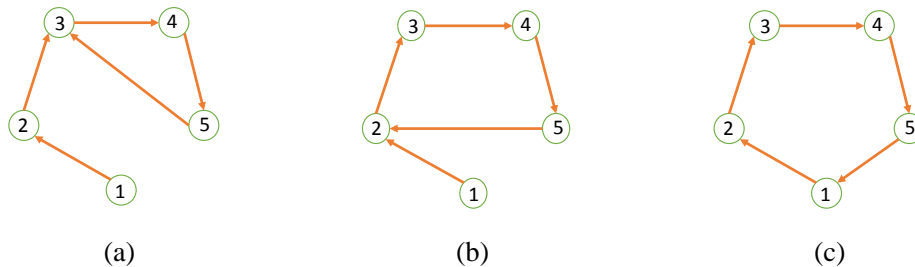


Figure 3: Different rehypothecation process among five banks: same number of links, different lengths of cycles but same total amounts of equilibrium collateral.

<sup>14</sup>It is also possible to show that, as long as all agents have positive out-degree, collateral flows will end up in a cycle after a finite number of steps. For the sake of brevity we do not report this proposition and the related proof. However, it is available from the authors upon request.

Let us next consider three other examples of rehypothecation process among five banks, the ones in Figure (4). The difference with the examples of Figure 3 is that now in panels (a) and (b) one node (i.e. node 5) has zero out-degree. In addition, the network structure in these two panels imply that some collateral leaks out of a cycle and gets stuck at the node with zero out-degree, which then plays the role of “collateral sink”. The consequence is that the three networks will generate different amounts of total collateral in equilibrium. This is stated in the following proposition.

**Proposition 2.** Let  $\theta_i = \theta$  ( $\forall i$ ). For the networks in panels  $\alpha = a, b, c$  of Figure 4,  $S_{a,t}^{out} < S_{b,t}^{out} < S_{c,t}^{out}$  ( $\forall t \geq 2$ ).

*Proof.* See appendix. □

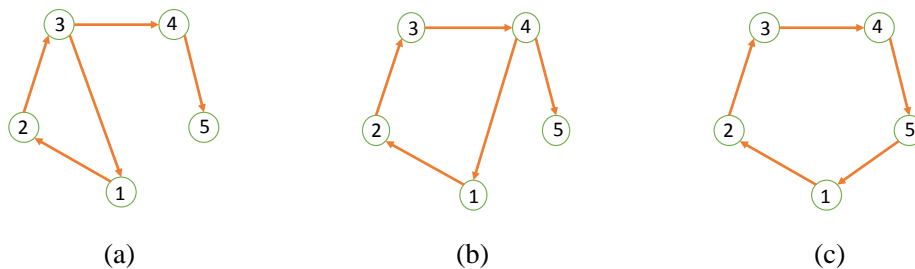


Figure 4: Different rehypothecation process among five banks: same number of links but different total amounts of equilibrium collateral.

The above two propositions deliver interesting implications about the role of networks’ topology in determining collateral flows. First, proposition 2 shows that total collateral is maximized when the longest possible cycle in the network has been created (a cycle of length 5 in example (c) of Figure 4). At the same time, Proposition 1 shows that cycles’ length is irrelevant when collateral sinks are not present in the network and all banks have positive out-degree, i.e. they have at least one repo with some other bank in the system. In this case, it might be advantageous to concentrate collateral flows among few nodes that have a cyclic chain among them. These results provide key insights to understand the behaviour of collateral flows in different network architectures that we shall discuss in the next section. They are also central to understand some of the results about collateral hoarding cascades that we will expose in Section 5. As a final note, it is important to stress that chains, cycles and collateral sinks must be considered as strongly related concepts. Indeed, breaking cycles would either increase the length chains or the number of collateral sinks. Likewise, reducing collateral sinks would increase the length of chains or it would create cycles.

The next two propositions generalize the above results to any network architecture. The first of them shows that adding an arbitrary number of links to a cycle of length equal to the size of the network does not change either total collateral or the value of the multiplier. The second one identifies the upper bounds for the equilibrium values of total collateral and of the multiplier and it shows that these upper limits are attained as long as every bank has at least one outgoing link in the network.

**Proposition 3.** Consider a rehypothecation network  $\mathcal{G}$  of size  $N$ . Let  $\theta_i = \theta$  ( $\forall i$ ) and  $A_i^0 = A^0$  ( $\forall i$ ). If  $k_i^{out} > 0$  ( $\forall i$ ) then equilibrium values of  $S^{out}$  and  $m$  are equal to the following upper limits:

$$S^{out} = \frac{\theta}{1 - (1 - h)\theta} NA^0,$$

and

$$m = \frac{1}{1 - (1 - h)\theta}.$$

*Proof.* See the appendix. □

**Proposition 4.** Consider a rehypothecation network  $\mathcal{G}$  of size  $N$ . Let  $\theta_i = \theta$  ( $\forall i$ ) and  $A_i^0 = A^0$  ( $\forall i$ ). Adding arbitrary links to an initial cycle of size  $N$  does not change the values of  $S^{out}$  and  $m$ . More in general, as long as there is the presence of the largest cycle,  $S^{out}$  and  $m$  remain unchanged as the density inside that cycle increases.

*Proof.* See the appendix. □

### 3.3 Network architecture and collateral multiplier

We now address the issue of how the network structure more in general affects collateral dynamics in presence of rehypothecation. We shall focus on three very different paradigmatic network architectures that are well established in the literature. Although these structures alone may not describe well the empirical features of real-world networks, they capture some idealized modes of organization of financial contracts in the market. Moreover, they allow one to clearly highlight the role played in real-world collateral networks (see e.g. Baranova et al., 2016; Keller et al., 2014; Aguiar et al., 2016) by link heterogeneity and concentration in the determination of the collateral multiplier.

The first network structure we consider is the closed  $k$ -regular graphs of size  $N$ ,  $\mathcal{G}_{reg}$ , wherein each node has  $k$  in-coming neighbors as well as  $k$  out-going neighbors. This archetype corresponds to a market where repo contracts are homogeneously spread across banks, so that each bank has exactly the same number of repos and of reverse repos. We consider different types

of closed regular graphs of varying levels of density  $\frac{1}{N-1} < p < 1$ . Special cases of this structure are the cycle of size  $N$  (where  $p = 1/(N - 1)$ ) and the complete network ( $p = 1$ ), wherein each bank has a repo with every other bank in the network (and vice-versa) and where the number of incoming and outgoing links is equal to  $N - 1$ . In the second structure we consider, the random graphs  $\mathcal{G}_{rg}$ , we introduce a mild degree of heterogeneity in the distribution of financial contracts across banks, by assuming that the probability of a directed link (and thus of the existence of repo) between every two nodes is equal to the density of the network  $p$  ( $0 \leq p \leq 1$ ). Notice that as  $p \rightarrow 1$  the random graph converges to the complete graph, i.e. the graph where every bank is connected to every other bank and vice versa. Finally, the third architecture we examine are core-periphery networks,  $\mathcal{G}_{cp}$ , where (i) the number of nodes in the core,  $N_{core}$ , is fixed; (ii) each node in the periphery has only out-going links, all pointing to nodes in the core; (iii) nodes in the core are also randomly connected among themselves with probability  $p_{core}$  ( $0 \leq p_{core} \leq 1$ ), and there are no directed links from the core to the periphery nodes. Notice that the latter type of structure exacerbates heterogeneity in the distribution of financial contracts and it centralizes collateral flows among nodes in the core. This structure is also interesting from an empirical viewpoint as high concentration of collateral flows is often observed in actual markets (see e.g. Baranova et al., 2016).

We begin our analysis of the three structures by characterizing equilibrium total collateral and the corresponding multiplier in the closed k-regular graphs.

**Proposition 5.** Let  $\theta_i = \theta \ \forall i$  and  $A_i^0 = A^0 \ \forall i$ . A closed-k regular rehypothecation network  $\mathcal{G}_{reg}$  of size  $N$ , and a density  $p = \frac{k}{N-1}$ , always returns the same equilibrium values of total collateral  $S_{reg}^{out}$  and of collateral multiplier  $m_{reg}$  for any density  $\frac{1}{N-1} < p < 1$ . The equilibrium values are given by the limits stated in Proposition 3.

*Proof.* The above statement follows directly from Proposition 4 above. □

A closed k-regular graph of density  $\frac{1}{N-1}$  already embeds the longest possible cycle that is possible to create in a network of size  $N$ . Accordingly, adding further links does not bring any change in equilibrium values of total collateral and of the multipliers, which are always equal to the upper bounds stated in Proposition 3. In contrast to the closed k-regular graph, the random network and the core-periphery networks display some variation in total collateral and in the multiplier with increasing levels of density. The following proposition characterizes the behavior of the latter two variables in these two network structures.<sup>15</sup>

---

<sup>15</sup>In the next proposition we determine the equilibrium for bank's collaterals in the case of an average system, that is instead of considering each single sample of collateral networks we consider the expected value of the amount of collateral for each banks, and solve only for a single average system. Numerical results strongly supports the analytic ones for all cases considered.

**Proposition 6.** Let  $\theta_i = \theta \ \forall i$  and  $A_i^0 = A^0 \ \forall i$ , then:

1. A random graph  $\mathcal{G}_{rg}$  of size  $N$  creates more equilibrium collateral and a higher multiplier with higher level of density  $p$ .
2. A core-periphery graph of  $\mathcal{G}_{cp}$  of size  $N$  creates more equilibrium collateral and a higher multiplier with higher level of density  $p$ .
3. Let  $p_{core}$  be the density of the core in a core-periphery graph  $\mathcal{G}_{cp}$  of size  $N$  and with a core of size  $N_{core}$ . For any graph density  $0 \leq p \leq 1$ ,  $\exists p_{th} = p_{th}(N, N_{core}, p)$  such that, if  $p_{core} > p_{th}$ , then the core-periphery graph  $\mathcal{G}_{cp}$  creates more equilibrium collateral and a higher multiplier than a random graph  $\mathcal{G}_{rg}$  of size  $N$  and density  $p$ .
4. As  $p \rightarrow 1$  the equilibrium values of total collateral and the multiplier of the random graph  $\mathcal{G}_{rg}$  and of the core-periphery graph  $\mathcal{G}_{cp}$  converge to the limits stated in Proposition 3.

*Proof.* See the appendix. □

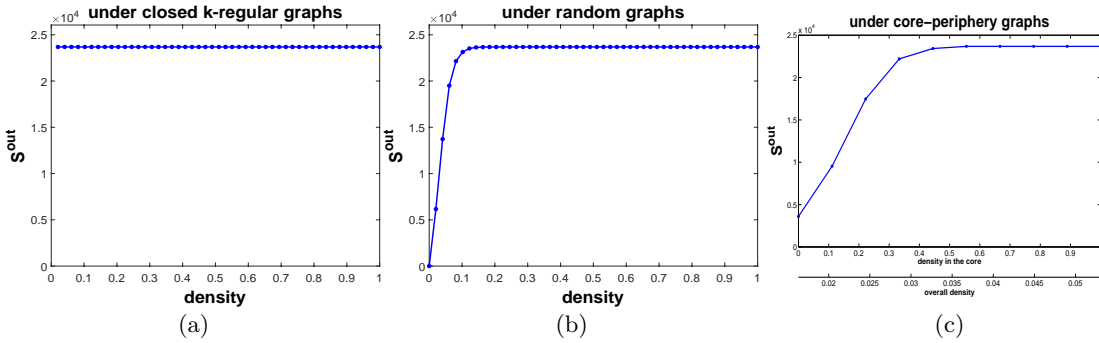


Figure 5: Total collateral ( $S^{out}$ ) as a function of density under different network structures.

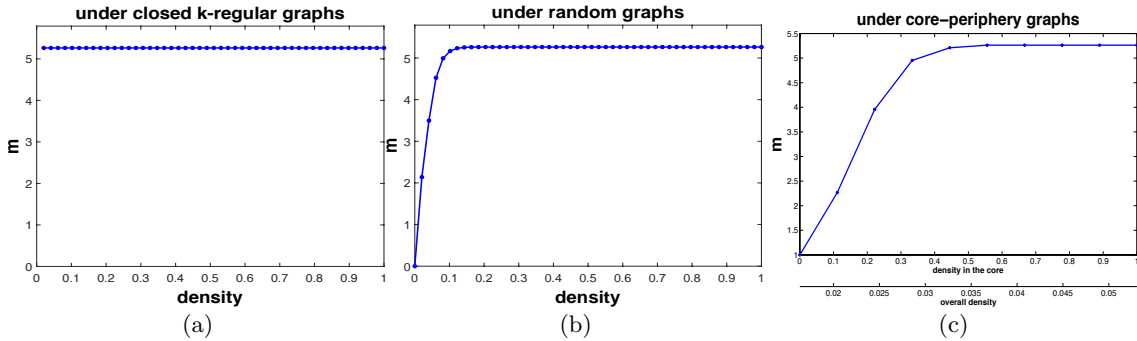


Figure 6: Collateral multiplier ( $m$ ) as a function of density under different network structures.

The plots in Figures 5 and 6 help to visualize the results contained in the last two propositions. The plots show equilibrium values of total collateral and of the multiplier resulting from numerical simulations<sup>16</sup> using each of the three network topologies examined above (closed k-regular, random graph, and core-periphery) and with different levels of density. Notice that in display (c) both the scale of density of the core  $p_{core}$  and the overall density are shown.<sup>17</sup> First, the plots show that both total collateral and the multiplier do not change with the level of density in the closed k-regular graph (plot (a) in both figures). In contrast, both variables increase with the level of density in the random graph and in the core-periphery network (respectively, panels (b) and (c) of the two figures), before eventually converging to the same value of the closed k-regular graph (and determined by the expressions in Proposition 3). The decrease of the collateral multiplier for low density in random graphs and core-periphery graphs is related to the emergence of collateral sinks: such an effect is not observed in regular graphs where collateral sinks are not present. The main intuition for the latter result is that increasing the level of density (in the overall network or in the core) increases both the number and the length of cycles in the network<sup>18</sup>. These two factors have a positive impact on the liquidity created by the network, as we explained in Section 3.2. However, when the longest possible cycle in the network (for the random graph) or in the core (for the core-periphery graph) adding further links does not increase liquidity. Furthermore, both the third statement of Proposition 6 and the plots in the figures indicate the core-periphery network generates a much higher total collateral than the random graph with small changes in network density. For instance the inspection of Figure 7 reveals that with  $N = 50$  banks in the network a tiny increase in overall density (from 0.02 to 0.03) has the effect of more than doubling the value of the multiplier (from 2 to almost 5). In contrast, a much larger change in density is required to produce a similar effect in the random graph. This result generalizes the insights discussed in the previous section (cf. Proposition 1). Once all banks have positive out-degree and they are thus all contributing with outflowing collateral - i.e. collateral sinks are absent - concentrating all collateral flows in a small cycle (like the one in the core) already generates the largest possible total collateral. It is important

---

<sup>16</sup>The numerical simulation is implemented with  $N = 50$ ,  $1 - \theta = 0.1$ ,  $A^0 = 100$  and an haircut rate  $h = 0.1$  for all banks. The study of Copeland et al. (2012) provides some descriptive statistics on haircut on (tri-party) repos. The median haircut applied to U.S. Treasuries was 2%, while the median haircuts on corporate bonds and equities were 5% and 8%, respectively. In our paper, focusing on the bilateral repos, we assume that the haircut is constant and slightly higher with  $h = 10\%$ . In fact, as shown in Gorton and Metrick (2012), the haircut rate in bilateral repo markets can vary in a broader range: (i) the average haircut reached to nearly 50% at the peak of the crisis in late 2008; and (ii) several classes of assets were stopped entirely from being used as collateral, an unprecedented event that is equivalent to a haircut of 100%.

<sup>17</sup>Note that for the sake of simplicity and for the illustration purpose, in all numerical simulations for core-periphery graphs throughout this paper, we assume that  $\frac{N_{core}}{N} = 20\%$ , where  $N_{core}$  is the number of nodes in the core.

<sup>18</sup>In addition, for the random graph, the number of nodes with positive out-degree also increases with density, something which is consistent with the decrease in the number of collateral sinks that we stressed above.

to stress that the absence of collateral sinks is key for the above results concerning collateral multipliers in random and in core-periphery graphs and, relatedly, for the presence of advantages associated to links' concentration. Having instead collateral sinks in the network, e.g. by having collateral flows pointing from nodes in the core towards isolated nodes in the periphery would generate a lower collateral multiplier in core-periphery than in the random graphs.

The above results have implications for markets' organization, they indicate that the concentration of collateral flows among few nodes has, under some conditions, great advantages for collateral velocity and thus for the overall liquidity of the market. At the same time, in the next section we shall show that - when liquidity hoarding externalities are present - networks with highly concentrated collateral flows are also more exposed to larger collateral hoarding cascades following small local shocks.

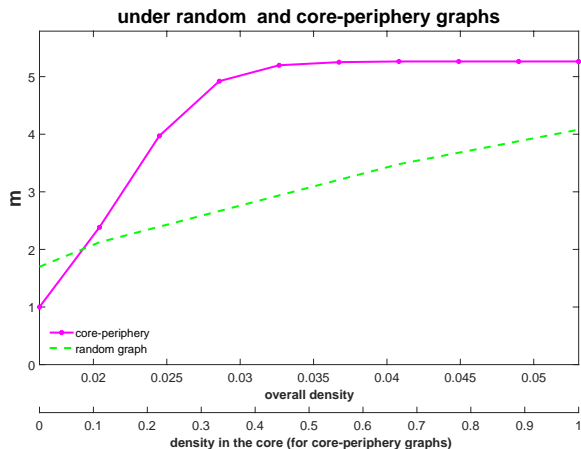


Figure 7: Collateral multiplier ( $m$ ) as a function of density in the random graph and in the core-periphery network.

## 4 The Extended Model: Value at Risk and Collateral Hoarding

So far we have worked with the assumption that non-hoarding rates  $\{\theta_i\}_{i=1}^N$  were constant across time and homogeneous across banks. This has simplified the analysis and it has allowed us to highlight the role of the characteristics of network topology in determining collateral flows in the financial system. At the same time, this hypothesis is also quite restrictive as banks' hoarding and non-hoarding might be responsive to the liquidity risk situation of banks and to the level of available collateral (see e.g. Acharya and Merrouche, 2010; Berrospide, 2012; de Haan and van den End, 2013). In addition, recent accounts of collateral dynamics (Singh, 2012) have documented the sizeable reduction in velocity of collateral in the aftermath of the last financial

crisis as a result of increased collateral hoarding by banks. To account for these important phenomena, in this section we extend the basic model presented in Section 2 to introduce time-varying non-hoarding rates determined by liquidity risk considerations.<sup>19</sup>

Again, to keep the model as simple as possible, we abstract from many important aspects concerning the banks' liquidity position. We assume that all funding is secured. For every bank  $j$  let  $NL_j$  be its net liquidity position. Recall that the amount of pledgeable collateral of bank  $j$  that can be used to get external funds with a haircut  $h$  is  $A_j^C$ . At the same time, if  $L_j \neq \emptyset$ , a fraction  $\theta_j$  of this amount of collateral is already pledged (i.e. an amount of  $A^{Cout} = \theta_j A_j^C$ ). The net liquidity position of bank  $j$  is thus given by:

$$NL_j = (1 - h)(1 - \theta_j)A_j^C(\theta_1, \theta_2, \dots, \theta_N, A^0, \mathcal{G}) - \epsilon_j, \quad (31)$$

where  $\epsilon_j$  are payments within the periods, which are assumed to be a i.i.d. normally distributed random variable with mean  $\mu_j$  and standard deviation  $\sigma_j$ . The notation  $A_j^C(\theta_1, \theta_2, \dots, \theta_N, A^0, \mathcal{G})$  emphasizes the fact that the total collateral position of a bank depends also on the fractions of non-hoarded collateral of all banks in the network  $\mathcal{G}$ . Notice that the above equation implies that the more borrowers of  $j$  hoard collateral, the lower is the value of collateral  $A_j^C$ , and thus the higher the need to hoard collateral for  $j$ .

Let us start by observing that a realization of the liquidity shock that is sufficiently high may imply the default of bank  $j$ . This occurs when

$$\epsilon_j > (1 - h)(1 - \theta_j)A_j^C.$$

Given the assumption on the random variable  $\epsilon_j$ , default is an event occurring with probability

$$\text{prob.}(NL_j < 0) = \text{prob.}(\epsilon_j > (1 - h)(1 - \theta_j)A_j^C).$$

Furthermore, following Adrian and Shin (2010) and Adrian and Shin (2014), we assume that each bank  $j$  employs a Value-at-Risk (VaR) strategy to determine the fraction of collateral to hoard, so that the above probability of default is not higher than a target  $(1 - c_j)$  (where  $0 < c_j < 1$ ). We can see that  $\theta_j$  depends not only on the uncertainty about  $\epsilon_j$  but also on the haircut rate  $h$  and, finally, on the value of the collateral  $A_j^C$ . The interdependence between

---

<sup>19</sup>Velocity of collateral can also decrease because of higher haircut rates following an increase in counterparty risk (see Gorton and Metrick, 2012; Singh, 2012). Modelling haircut rates that reflect heterogenous counterparty risk would have increased the complexity of our model without affecting its basic results. In particular, an increase (decrease) in haircut rates have the same effect in the model as an increase (decrease) in collateral hoarding rates. And the factors that imply an increase in collateral hoarding rates (e.g. an adverse liquidity shock to some nodes) are in general positively correlated with the factors that generate an increase in counterparty risk and thus in haircut rates.

$\theta_j$  and  $A_j^C$  implies that each bank will adjust its hoarding preference (i.e. hold more or less collateral) in anticipation of expected “losses” or “gains” in its total amount of collateral. It also follows that a change in hoarding rates at bank  $j$  will induce a change in hoarding rates at the banks to which  $j$  is connected to.

If we assume that returns on external assets held by  $j$  are higher than the repo rate, then each bank  $j$  will decide the optimal fraction  $\theta_j$  such that

$$\text{prob.}(\epsilon_j > (1-h)(1-\theta_j)A_j^C) = 1 - c_j. \quad (32)$$

Given that  $\epsilon_j$  are a i.i.d. normally distributed random variable we have

$$\text{prob.}(NL_j < 0) = \text{prob.}(\epsilon_j > (1-h)(1-\theta_j)A_j^C) = \frac{1}{2} \left[ 1 - \text{erf}\left(\frac{(1-h)(1-\theta_j)A_j^C - \mu_j}{\sigma_j\sqrt{2}}\right) \right], \quad (33)$$

where erf is the Gauss error function defined as

$$\text{erf}(x) = \frac{1}{\pi} \int_{-x}^x e^{-t^2} dt. \quad (34)$$

Under the VaR constraint, bank  $j$  sets the share of hoarded collateral at the level  $\theta_j^*$  such that

$$\frac{1}{2} \left[ 1 - \text{erf}\left(\frac{(1-h)(1-\theta_j)A_j^C - \mu_j}{\sigma_j\sqrt{2}}\right) \right] = 1 - c_j \quad (35)$$

$\Leftrightarrow$

$$\text{erf}\left(\frac{(1-h)(1-\theta_j)A_j^C - \mu_j}{\sigma_j\sqrt{2}}\right) = 2c_j - 1 \quad (36)$$

$\Leftrightarrow$

$$\theta_j = 1 - \frac{\sigma_j\sqrt{2}\text{argerf}(2c_j - 1) + \mu_j}{(1-h)A_j^C}, \quad (37)$$

where argerf is the inverse error function defined in  $(-1, 1) \rightarrow \mathbb{R}$  such that

$$\text{erf}(\text{argerf}(x)) = x. \quad (38)$$

Equation (37) indicates that  $\theta_j$  is a decreasing function of the VaR target  $c_j$ , of the uncertainty about the liquidity shock (captured by  $\sigma_j$ ), of the mean of the liquidity shock  $\mu_j$ , and of the haircut rate  $h$ . Moreover, it is an increasing function of the value of the collateral  $A^C$  and of the shares of non-hoarded collateral of other banks in the network. Denote

$$c_j^0 = \sigma_j\sqrt{2}\text{argerf}(2c_j - 1) + \mu_j, \quad (39)$$

we then obtain the following final expression for the optimal  $\theta_j$  under the assumption of normally-distributed liquidity shocks:

$$\theta_j = 1 - \frac{c_j^0}{(1-h)A_j^C(\theta_1, \theta_2, \dots, \theta_N, A^0, \mathcal{G})}. \quad (40)$$

We now investigate the existence of equilibrium in non-hoarding rates. From Equation (40) it follows that the hoarding rate  $(1-\theta_j)$  of a bank  $j$  can be expressed as:

$$(1-\theta_j) = \frac{c_j^0}{(1-h)A_j^C(\theta_1, \theta_2, \dots, \theta_N, A^0, \mathcal{G})}, \quad (41)$$

where the variable  $c_j^0$  defined by equation (39) captures the effects of uncertainty in  $\epsilon_j$  on  $(1-\theta_j)$ . If we assume that  $\theta_j$  is defined on the closed interval  $[0, 1]$  ( $\theta_j \in [0, 1]$ ) then  $A_j^C(\theta_1, \theta_2, \dots, \theta_N, A^0, \mathcal{G})$  must be in  $[\frac{c_j^0}{1-h}, \infty]$ . From equation (41), it follows that

$$(1-h)\theta_j = \frac{(1-h)A_j^C - c_j^0}{A_j^C}. \quad (42)$$

Equivalently,

$$(1-h)\frac{\theta_j}{k_j^{out}} = \frac{(1-h)A_j^C - c_j^0}{A_j^C k_j^{out}}, \quad (43)$$

where  $k_j^{out}$  is the outdegree of bank  $j$ . Recall that, under the assumption that banks homogeneously spread collateral across their lenders, we have:

$$w_{i \leftarrow j} = \theta_j s_{i \leftarrow j} = \frac{\theta_j}{k_j^{out}}, \quad \forall i \in L_j \neq \emptyset.$$

Therefore,

$$(1-h)w_{i \leftarrow j} = \frac{(1-h)A_j^C - c_j^0}{A_j^C k_j^{out}}, \quad \forall i \in L_j \neq \emptyset.$$

Next, denote by  $\tilde{\mathcal{W}}^{VaR} = \{\tilde{w}_{i \leftarrow j}\}$  the matrix with size  $N \times N$  where

$$\begin{cases} \tilde{w}_{i \leftarrow j} = \frac{(1-h)A_j^C - c_j^0}{A_j^C k_j^{out}}, \quad \forall i \in L_j \neq \emptyset, \\ \tilde{w}_{i \leftarrow j} = 0, \quad \text{elsewhere.} \end{cases} \quad (44)$$

The level of collateral  $A_i^C$  is then obtained by solving the following equation

$$A_i^C = A_i^0 + \sum_{j \in B_i} \tilde{w}_{i \leftarrow j} A_j^C, \quad \forall i = 1, 2, \dots, N. \quad (45)$$

Finally, the non-hoarded rates  $\theta_i$  can be obtained by substituting  $A_i^C$  into equation (42).

In general, the solution to the system composed by the system of equations in (45) might not be unique. However, in the following proposition we establish sufficient conditions for the uniqueness of the solution of that system.

**Proposition 7.** If  $0 < h < 1$  and  $\tilde{\mathcal{A}}^{-1}\tilde{\mathbf{b}} \geq \frac{\mathcal{C}^0}{1-h}$  where  $\mathcal{C}^0 = [c_1^0, c_2^0, \dots, c_{N-1}^0, c_N^0]^T$  is a column vector captures the effects of the net liquidity shock on hoarding preference, then the system (45) has a single unique solution<sup>20</sup>

$$A^C = \tilde{\mathcal{A}}^{-1}\tilde{\mathbf{b}}, \quad (46)$$

where  $\tilde{\mathbf{b}}$  is a column vector size  $N \times 1$ , given by

$$\tilde{\mathbf{b}} = A^0 - \mathcal{S}\mathcal{C}^0 \quad (47)$$

and the matrix  $\tilde{\mathcal{A}} = \{\tilde{a}_{i \leftarrow j}\}$  with size  $N \times N$ , defined as

$$\tilde{\mathcal{A}} = I - (1 - h)\mathcal{S}. \quad (48)$$

*Proof.* See the appendix. □

Finally, by substituting  $A^C$  in (46) into equation (42), we obtain the solution to the equilibrium rates of non-hoarded collateral as follows

$$\theta_j = 1 - \frac{c_j^0}{(1-h)\tilde{\mathcal{A}}^{-1}\tilde{\mathbf{b}}}. \quad (49)$$

In the next section, we use the above results about the determination of equilibrium banks' collateral  $A_j^C$  and non-hoarding rates  $\theta_j$  to study the emergence of collateral hoarding cascades under different network structures.

---

<sup>20</sup>Throughout this paper, for any two vectors  $X$  and  $Y$  of size  $n \times 1$  ( $n \geq 1$ ), then  $X \geq Y$  if  $X_i \geq Y_i, \forall i = 1, \dots, n$ .

## 5 Collateral hoarding cascades

We now use the VaR collateral hoarding model developed in the previous section to study how different rehypothecation networks react when a fraction of banks is hit by adverse shocks. We focus on uncertainty shocks<sup>21</sup> that cause the variable  $c_i^0$  in Equation (40) to increase to  $c_i^1 = c_i^0(1 + \tilde{c}^0)$  for some banks  $i$ , where  $\tilde{c}^0 \geq 0$ . The shock leads those banks to increase their hoarding of collateral. This in turn triggers a cascade of hoarding effects at banks that are either directly or indirectly connected to the banks initially hit by the shock. Indeed, higher hoarding at bank  $i$  also causes a loss in the collateral flowing into bank's  $i$  neighbors. As a consequence, the latter banks also increase their hoarding rates, causing further losses in collateral inflows at other banks in the system and thus further adjustments in hoarding rates. The final result of the foregoing cascade is a new equilibrium characterized, in general, by a lower level of total collateral in the system. On the grounds of the results stated in Proposition 7 we can determine the new equilibrium vector of collateral in the aftermath of a local uncertainty shock. More formally, let  $\mathcal{C}^1 = [c_1^1, c_2^1, \dots, c_{N-1}^1, c_N^1]^T$  the new vector of uncertainty factors in the aftermath of such a shock. By substituting  $\mathcal{C}^1$  into equations (46) and (47), we obtain the new equilibrium solution,  $A^{C^1}$ , to  $A^C$  at the end of the hoarding cascade as follows

$$A^{C^1} = \tilde{\mathcal{A}}^{-1}[A^0 - \mathcal{S}\mathcal{C}^1]. \quad (50)$$

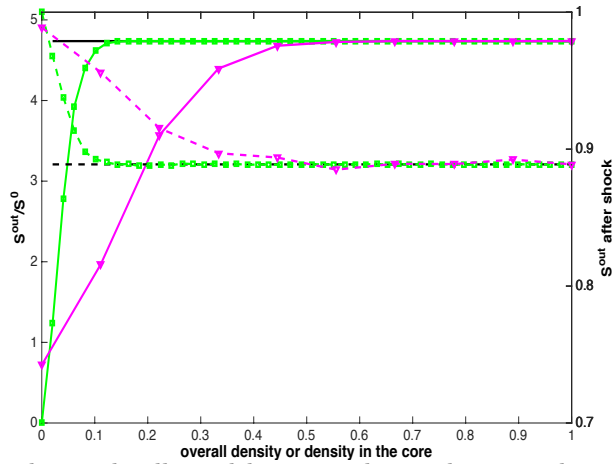


Figure 8: Collateral multiplier and collateral losses in the random attack scenario. In each panel, the left y-axis shows the ratio between total outflowing collateral and total proprietary collateral  $S^{out}/S^0$  (solid line). The right y-axis shows total collateral  $S^{out}$  after shock (relative to the pre-shock level, dashed line). Different network structures are represented by different colors and markers: closed k-regular graph (black, no marker), random graphs (green, squares), core-periphery graphs (magenta, diamonds).

<sup>21</sup>We also performed analysis of the impact of aggregate shocks to the value of collateral. However, results and the dynamics were similar to the one reported in the paper.

To study the impact of the above local uncertainty shocks on equilibrium collateral in different networks, we calculate equilibrium collateral before and after a fraction  $f = 20\%$  of banks in a given network experiences a 50% increase in the uncertainty factor (so that  $\tilde{c}^0 = 0.5$ ). We consider the same network structures studied in Section 3.3 and two different shocks scenarios. In the first scenario, that we label “random attack”, the banks hit by the uncertainty shock are randomly selected. In the second scenario, that we label “target attack”, the shocked banks are selected according to their centrality<sup>22</sup> in the network (in descending order).<sup>23</sup> Notice that this second shock scenario is relevant only for the random networks and for the core-periphery networks, as all nodes have the same centrality in a closed k-regular network.

Figure 8 refers to numerical results in the random attack scenario. It shows, on the left-scale, the pre-shock levels of the ratio between equilibrium total collateral  $S^{out}$  and total proprietary collateral  $S^0$ . The right scale shows instead the equilibrium total collateral after the shock (relative to its pre-shock value). The two variables are plotted as a function of network density and for the three different structures examined in the section 3.3, namely the closed k-regular networks  $\mathcal{G}_{reg}$ , the random networks  $\mathcal{G}_{rg}$ , and the core-periphery networks  $\mathcal{G}_{cp}$ .

Figure 8 reveals first that - before the shock - the behaviour of total collateral as a function of network density is the same as the one discussed in Section 3.3 for the case of constant hoarding rates<sup>24</sup>. Total equilibrium collateral increases with density in the random graphs and in the core-periphery graphs, whereas it stays constant with density in closed k-regular graphs. Accordingly, it is not surprising that the local uncertainty shock has some effects only in the random networks and in the core-periphery networks. In particular, the comparison of the two lines on the left- and right-scales of the figure indicates that the foregoing two networks display a trade-off between liquidity and systemic (liquidity) risk. Increasing density in these networks allows significant increases in collateral velocity and in endogenous capacity. At the same time, it makes the financial system exposed to aggregate liquidity losses in presence of small local shocks.

---

<sup>22</sup>We use “PageRank” centrality (see Newman, 2010; Battiston et al., 2012, for more details). However, the main conclusions still hold when the degree centrality is employed.

<sup>23</sup>The other parameters of the simulation were set so that the number of banks is  $N = 50$ ,  $A_i^0 = 100$ ,  $1 - \theta_i = 0.1$  and  $c_i^0 = 1$  and  $h = 0.1$  for all banks. About the haircut rate  $h$ , the study of Copeland et al. (2012) provides some descriptive statistics on haircut on (tri-party) repos. The median haircut applied to U.S. Treasuries was 2%, while the median haircuts on corporate bonds and equities were 5% and 8%, respectively. In our paper, focusing on the bilateral repos, we assume that the haircut is constant and slightly higher with  $h = 10\%$ . In fact, as shown in Gorton and Metrick (2012), the haircut rate in bilateral repo markets can vary in a broader range: (i) the average haircut reached to nearly 50% at the peak of the crisis in late 2008; and (ii) several classes of assets were stopped entirely from being used as collateral, an unprecedented event that is equivalent to a haircut of 100%.

<sup>24</sup>Indeed, all the results of Propositions 5 and 6 hold also in the model where hoarding rates are determined according to a VaR criterion. For the sake of brevity, we do not report here these propositions and the related proofs. However, they are available from the authors upon request.

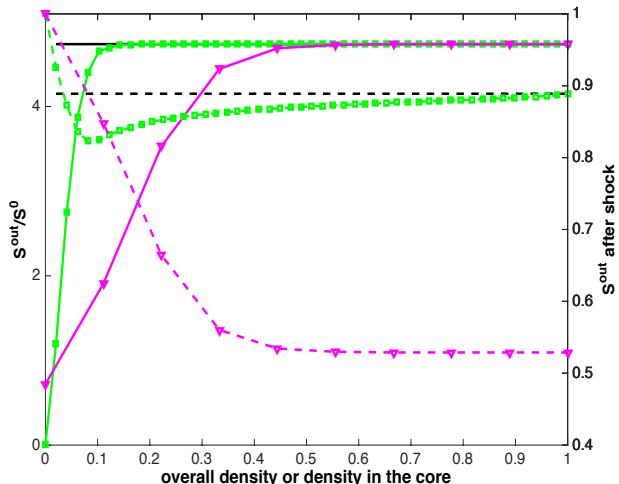


Figure 9: Collateral multiplier and collateral losses in the target attack scenario. In each panel, the left y-axis shows the ratio between total outflowing collateral and total proprietary collateral  $S^{out}/S^0$  (solid line). The right y-axis shows total collateral  $S^{out}$  after shock (relative to the pre-shock level, dashed line). Different network structures are represented by different colors and markers: closed k-regular graph (black, no marker), random graphs (green, squares), core-periphery graphs (magenta, diamonds).

Figure 8 also indicates the maximal impact is quite small (only a 10% loss), and that both the random and core-periphery networks generate the same aggregate loss in total collateral as overall density converges to 1. How do these results change when one switches from random to target attacks based on nodes centrality?

Figure 9 reproduces the same plots as in Figure 8, but now considering the the target attack scenario, i.e. the one where the banks that hit by the shocks are those with the highest centrality in the network. The plots indicate, again, that the random and core-periphery display a trade-off between liquidity and systemic risk as density increases. Nevertheless, the maximal loss generated in core-periphery networks is much larger (up to 50% of the initial total collateral value).

Thus, the core-periphery network generates very large losses in collateral when central nodes are hit by local uncertainty shocks. Recall that those nodes are precisely the ones concentrating collateral flows, and thus generating the large increases in liquidity stressed in Section 3.3. On the one hand, concentrating collateral flows generates large gains in market liquidity with a low network density. On the other hand, high concentration produces large liquidity losses when small local shocks come across. Indeed, by concentrating collateral flows, more central nodes have also a larger impact on collateral at the peripheral nodes that have connections with them. They thus trigger a stronger adjustment in hoarding rates thereafter. Notice that these concentration effects underlying large liquidity losses in the core-periphery network are

much smaller in the random graph (where link heterogeneity is small). In addition, they are completely absent in the closed  $k$ -regular graph, where all nodes have the same centrality.

To conclude, it is useful to stress that liquidity hoarding externalities play a key role in the generation of the significant trade-off between liquidity and systemic risk observed in core-periphery networks. In other terms, targeted local shocks would have a small impact in core-periphery networks if hoarding rates were not responsive to changes in the liquidity positions of banks. To understand why, notice that with constant hoarding rates a loss in collateral value or an exogenous increase in hoarding rates at one bank  $i$  will only have a  $n^{\text{th}}$ -order effect at neighbouring banks as the initial shock is dampened by haircut rates and hoarding rates at other banks along the collateral chain. For instance, in the very simple case of the cycle (i.e. closed chain) displayed in Figure 1 (c) a shock to outflowing collateral at node 1 ( $A_1^{\text{out}}$ ) will only have an effect of order  $\theta_3(1-h)\theta_2(1-h)$  on outflowing collateral at node 3 (see also Equation (25)). In the case of VaR-determined hoarding rates the effect is not small because it is reinforced by a revision in hoarding rates at each step along the chain.<sup>25</sup>

## 6 Concluding remarks

We have built and analyzed a simple model of collateral flows over a network of repo contracts among banks. We have assumed that, to obtain secured funding, banks may pledge their proprietary collateral or re-pledge the collateral obtained by other banks via reverse repos. The latter practice is known as “rehypothecation” and it has clear advantages for market liquidity as it allows banks to secure more transactions with the same set of collateral. At the same time, re-pledging other banks’ collateral may also raise liquidity risk concerns, as several banks rely on the same collateral for their repo transactions. We have focused on investigating which characteristics of rehypothecation networks are key in order to increase the velocity of collateral flows, and thus increase the liquidity in the market. We have first assumed that banks hoard a constant fraction of their collateral. Under this hypothesis we have shown that characteristics of the network like the length of re-pledging chains, the presence of cyclic chains and collateral sinks and, finally, the direction of collateral flows are key determinant of collateral velocity and, accordingly, of the level of total collateral available for repo financing in the system. In particular, we have shown that collateral velocity increases with chains’ length. However, cyclic chains allow ceteris paribus a larger velocity than a-cyclic chains of the same length. Finally, we have shown that velocity is large already with small cyclic chains if the banks involved centralize collateral flows. The foregoing features of network topology underlie the results about the deter-

---

<sup>25</sup>In particular, in the example of Figure 1 (c) with VaR-based hoarding rates the effect of a shock to  $A_1^{\text{out}}$  on the outflowing collateral of node 3 be of the order  $(1-h)^2 \left( \theta_3\theta_2 + \theta_3 \frac{\partial\theta_2}{\partial A_1^{\text{out}}} + \theta_2 \frac{\partial\theta_3}{\partial A_1^{\text{out}}} \right)$ .

mination of total collateral and of collateral velocity in more general network architectures. In particular, we showed that velocity increases with density in the random network (displaying a mild heterogeneity in collateral flows across banks) and in the core-periphery networks (displaying high concentration of collateral flows). Nevertheless, core-periphery networks generate larger velocity than random networks already with smaller increase in the density of the network (as long as periphery nodes provide collateral to the core). The foregoing results have implications for the micro-structure of markets where collateral is important, as they highlight a new factor besides network density - i.e. concentration in collateral flows - that allows significant gains in market liquidity. A market with highly concentrated collateral flows generates higher velocity of collateral, as is thus more liquid, even if banks are not tied by a dense network of financial contracts.

Furthermore, we have extended the model to allow for hoarding rates that depend on the liquidity position of each bank in the network. More precisely, we assumed that banks set their hoarding rates by adopting a Value-at-Risk criterion aimed at minimizing the risk of liquidity defaults. We have shown that, in this framework, hoarding rates of each single bank are in general dependent by other banks' rates and collateral levels, a feature which introduces important collateral hoarding externalities in the analysis. We have then used the above framework to study the overall impact on collateral flows of local adverse shocks leading to an increase in payments' uncertainty at some banks in the market, in particular investigating how the response may vary with the topology of the rehypothecation network. We have highlighted that core-periphery networks where collateral flows are concentrated among nodes in the core generate larger losses in overall collateral compared to other network structures (closed k-regular networks, random networks) when the nodes experiencing the shock are the nodes in the core. This result has interesting implications for the regulatory analysis of markets with collateral, as it shows that the same network structures allowing for the largest increase in collateral velocity - i.e. core-periphery networks - are also the ones more exposed to large collateral hoarding cascades in case of small local shocks. A trade-off between liquidity and systemic (liquidity) risk thus emerges in those networks. In addition, our results also suggest that - in presence of rehypothecation - liquidity requirements imposed to banks need to account for the structure of the network of lending contracts across banks. In particular, such requirements should be dependent both on the systemic role of the banks in collateral flows (centrality), as well as for the whole topology of the network (presence of hierarchical structures like in the core-periphery architecture).

Our work could be extended at least in three ways. First, we have abstracted from several important aspects of real-world secured lending markets, such as heterogeneous quality of collateral and endogenous haircut rates, and the fact that collateral flows involve also non-banks actors (e.g. hedge funds on the supply side, and money market funds and other cash lenders on

the demand side). A more general analysis of collateral flows should try to include these aspects as well. Another factor that we did not model here is the “velocity drag” in collateral demand, considered e.g. in Duffie et al. (2015). Velocity drag weighs the daily standard deviation of the exposures towards individual counter-parties, and accounts for the unavailability of variation margin payments between the commitment and the actual deployment. This mechanism reduces the possibility of collateral re-use. Future work could try to account for such a delay in collateral transmission dynamics, e.g. by introducing a waiting time variable for the collateral that a counterparty has committed to pledge but has not yet effectively deployed.

Second, we have used the Value-at-Risk criterion to determine hoarding rates in our model. However, hoarding rates may also result from liquidity requirements imposed to banks. It would then be interesting to extend the model study how different requirements that have been proposed so far may impact on market liquidity in presence of rehypothecation, and how these requirements should be designed in order minimize the liquidity-systemic risk trade-off that we highlighted above. Finally, we have focused on bilateral repo contracts. However, it would be interesting to study how our results might change in presence of try-party repo structures, and in presence of central clearing counterparties that interact with banks re-using their collateral.

## Acknowledgments

We are indebted to three anonymous referees and to the editors of the Journal of Financial Stability. We also thank Joseph E. Stiglitz, Stephen G. Cecchetti, Sérafin Jaramillo, Dilyara Salakhova, Marco D’Errico, Guido Caldarelli, for valuable comments and discussions that helped to improve the paper. We also thanks participants to the various conferences where earlier versions of this paper were presented. These include the Second Conference on Network Models and Stress Testing for Financial Stability, Banco de México, September 26-27, 2017, the Conference on Complex System 2017 (CCS 2017), in Cancún, September 17-22, 2017, the first and second FINEXUS Conference, Zürich (January 2017, January 2018), the 22nd Workshop on Economic Science with Heterogeneous Interacting Agents (WEHIA 2017), Catholic University of Milan, June 12-14, 2017, and the 23rd Computing in Economics and Finance (CEF 2017), Fordham University, New York City, June 28-30, 2017. We also thank participants to seminars at the Jaume I University, Castellón de la Plana (Spain) in November 2017, to the Catholic University of Milan, in December 2017, and to the University of Florence, in March 2018. All usual disclaimers apply. The authors gratefully acknowledge the financial support of the Horizon 2020 Framework Program of the European Union under the grant agreement No. 640772 - Project DOLFINS (Distributed Global Financial Systems for Society).

## References

- Acemoglu, D., Ozdaglar, A., and Tahbaz-Salehi, A. (2015). Systemic Risk and Stability in Financial Networks. *American Economic Review*, 105(2):564–608.
- Acharya, V. and Merrouche, O. (2010). Precautionary hoarding of liquidity and inter-bank markets: Evidence from the sub-prime crisis. *Working Paper 16395*.
- Adrian, T. and Shin, H. S. (2010). Liquidity and leverage. *Journal of Financial Intermediation*, 19(3):418–437.

- Adrian, T. and Shin, H. S. (2014). Procyclical leverage and value-at-risk. *Review of Financial Studies*, 27(2):373–403.
- Aguiar, A., Bookstaber, R., Kenett, D. Y., and Wipf, T. (2016). A map of collateral uses and flows. *Journal of Financial Market Infrastructures*, 5(2):1–28.
- Andolfatto, D., Martin, F. M., and Zhang, S. (2017). Rehypothecation and liquidity. *European Economic Review*, 100:488–505.
- Baranova, Y., Liu, Z., and Noss, J. (2016). The role of collateral in supporting liquidity. Bank of England working papers 609, Bank of England.
- Bardoscia, M., Battiston, S., Caccioli, F., and Caldarelli, G. (2017). Pathways towards instability in financial networks. *Nature Communications*, 8:1–7.
- Barucca, P., Bardoscia, M., Caccioli, F., D’Errico, M., Visentin, G., Caldarelli, G., and Battiston, S. (2017). Network Valuation in Financial Systems. *ssrn.com/abstract=2795583*.
- Battiston, S., Farmer, J. D., Flache, A., Garlaschelli, D., Haldane, A. G., Heesterbeek, H., Hommes, C., Jaeger, C., May, R., and Scheffer, M. (2016). Complexity theory and financial regulation. *Science*, 351(6275):818–819.
- Battiston, S. and Martínez-Jaramillo, S. (2018). Financial networks and stress testing: Challenges and new research avenues for systemic risk analysis and financial stability implications. *Journal of Financial Stability*, 35:6–16.
- Battiston, S., Puliga, M., Kaushik, R., Tasca, P., and Caldarelli, G. (2012). Debtrank: Too central to fail? financial networks, the fed and systemic risk. *Scientific reports*, 2:541.
- Berrospide, J. (2012). Precautionary hoarding of liquidity and inter-bank markets: Evidence from the sub-prime crisis. *Working Paper*.
- Bottazzi, J.-M., Luque, J., and Páscoa, M. R. (2012). Securities market theory: Possession, repo and rehypothecation. *Journal of Economic Theory*, 147(2):477–500.
- Brunnermeier, M. K. and Pedersen, L. H. (2008). Market liquidity and funding liquidity. *The Review of Financial Studies*, 22(6):2201–2238.
- Capel, J. and Levels, A. (2014). Collateral optimisation, re-use and transformation: Developments in the dutch financial sector. *DNB Occasional Studies*, 12(5):1–54.
- Copeland, A., Duffie, D., Martin, A., and McLaughlin, S. (2012). Key mechanics of the us tri-party repo market. *Federal Reserve Bank of New York Economic Policy Review*, 18(3):17–28.
- Copeland, A., Martin, A., and Walker, M. (2014). Repo runs: Evidence from the tri-party pepo market. *The Journal of Finance*, 69(6):2343–2380.
- de Haan, L. and van den End, J. W. (2013). Banks responses to funding liquidity shocks: Lending adjustment, liquidity hoarding and fire sales. *Journal of International Financial Markets, Institutions and Money*, 26:152–174.
- Duffie, D., Scheicher, M., and Vuillemeij, G. (2015). Central clearing and collateral demand. *Journal of Financial Economics*, 116(2):237–256.
- Eisenberg, L. and Noe, T. H. (2001). Systemic Risk in Financial Systems. *Management Science*, 47(2):236–249.
- Financial Stability Board (2017a). Non-cash collateral re-use: Measure and metrics. 25 January:1–17.

- Financial Stability Board (2017b). Re-hypothecation and collateral re-use: Potential financial stability issues, market evolution and regulatory approaches. 25 January:1–42.
- Gai, P., Haldane, A., and Kapadia, S. (2011). Complexity, concentration and contagion. *Journal of Monetary Economics*, 58:453–470.
- Gorton, G. and Metrick, A. (2012). Securitized banking and the run on repo. *Journal of Financial economics*, 104(3):425–451.
- Gottardi, P., Maurin, V., and Monnet, C. (2017). A theory of repurchase agreements, collateral re-use, and repo intermediation. CESifo Working Paper Series 6579, CESifo Group Munich.
- Keller, J., Bouveret, A., Picillo, C., Liu, Z., Mazzacurati, J., Molitor, P., Sderberg, J., Theal, J., de Rossi, F., and Calleja, R. (2014). Securities financing transactions and the (re)use of collateral in europe an analysis of the first data collection conducted by the esrb from a sample of european banks and agent lenders. ESRB Occasional Paper Series 06, European Systemic Risk Board.
- Leitner, Y. (2011). Why do markets freeze? *Business Review, Federal Reserve Bank of Philadelphia*, (Q2):12–19.
- Monnet, C. (2011). Rehypothecation. *Business Review, Federal Reserve Bank of Philadelphia*, (Q4):18–25.
- Newman, M. (2010). *Networks: an introduction*. Oxford university press.
- Pozsar, Z. and Singh, M. (2011). The nonbank-bank nexus and the shadow banking system. Working Paper 11-289, International Monetary Fund.
- Rogers, L. C. G. and Veraart, L. A. M. (2013). Failure and rescue in an interbank network. *Management Science*, 59(4):882–898.
- Singh, M. (2011). Velocity of pledged collateral: analysis and implications. *IMF Working Paper 11/256*.
- Singh, M. (2012). The (other) deleveraging. *IMF Working Paper 12/179*.
- Singh, M. (2016). *Collateral and financial plumbing*. Risk Books.
- Visentin, G., Battiston, S., and D’Errico, M. (2016). Rethinking Financial Contagion. [ssrn.com/abstract=2831143](https://ssrn.com/abstract=2831143).

## 7 Appendix: Proofs of Propositions

### Proof for the existence of $\mathcal{B}_1$

To show that the matrix  $\mathcal{B}_1$  exists, we need to prove that  $\mathcal{I} - (1-h)\mathcal{M}$  is an invertible matrix. Using reductio ad absurdum method, let us assume that the matrix  $\mathcal{I} - (1-h)\mathcal{M}$  is not invertible, then  $\det(\mathcal{I} - (1-h)\mathcal{M}) = 0$ . Notice that this happens if and only if  $\frac{1}{1-h} (> 1)$  is an eigenvalue of  $\mathcal{M}$ . However, it can be easily show that the sum of all elements in each non-zero column of  $\mathcal{S}$  is less than or equal to  $\max(\theta_i) \leq 1$ . Hence, according to Perron-Frobenius theorem, the largest eigenvalue of  $\mathcal{S}$  cannot be larger than 1.

### Proof of proposition 1

Let us start by remarking that, in all cases shown in Figure (3), we have  $k_i^{out} > 0$  ( $\forall i = 1, 2, 3, 4, 5$ ), and thus  $\delta_i = 1$  ( $\forall i = 1, 2, 3, 4, 5$ ) and

$$\begin{cases} A_{1,t=1}^{Cout} = A_1^{0out} = \theta_1 A_1^0 \\ A_{2,t=1}^{Cout} = A_2^{0out} = \theta_2 A_2^0 \\ A_{3,t=1}^{Cout} = A_3^{0out} = \theta_3 A_3^0 \\ A_{4,t=1}^{Cout} = A_4^{0out} = \theta_4 A_4^0 \\ A_{5,t=1}^{Cout} = A_5^{0out} = \theta_5 A_5^0 \end{cases} \quad (51)$$

In the case of Figure 3 (a), the dynamics of  $\{A_{i,T}^{Cout}\}_{i=1}^5$  will follow

$$\begin{cases} A_{1,T+1}^{Cout} = A_1^{0out} \\ A_{2,T+1}^{Cout} = A_2^{0out} + (1-h)\theta_2 A_{1,T}^{Cout} \\ A_{3,T+1}^{Cout} = A_3^{0out} + (1-h)\theta_3 A_{2,T}^{Cout} + (1-h)\theta_3 A_{5,T}^{Cout} \\ A_{4,T+1}^{Cout} = A_4^{0out} + (1-h)\theta_4 A_{3,T}^{Cout} \\ A_{5,T+1}^{Cout} = A_5^{0out} + (1-h)\theta_5 A_{4,T}^{Cout} \end{cases} \quad (52)$$

We obtain

$$\begin{pmatrix} A_{1,T+1}^{Cout} \\ A_{2,T+1}^{Cout} \\ A_{3,T+1}^{Cout} \\ A_{4,T+1}^{Cout} \\ A_{5,T+1}^{Cout} \end{pmatrix} = \{I + [(1-h)M_a]^1 + [(1-h)M_a]^2 + \dots + [(1-h)M_a]^T\} \begin{pmatrix} A_1^{0out} \\ A_2^{0out} \\ A_3^{0out} \\ A_4^{0out} \\ A_5^{0out} \end{pmatrix}, \quad (53)$$

with

$$M_a = \begin{bmatrix} 0 & 0 & 0 & 0 & 0 \\ \theta_2 & 0 & 0 & 0 & 0 \\ 0 & \theta_3 & 0 & 0 & \theta_3 \\ 0 & 0 & \theta_4 & 0 & 0 \\ 0 & 0 & 0 & \theta_5 & 0 \end{bmatrix}.$$

In the case of Figure 3 (b), the length of the closed cycle is 4, and now the dynamics of  $\{A_{i,T}^{Cout}\}_{i=1}^5$  is governed by the following system

$$\begin{cases} A_{1,T+1}^{Cout} = A_1^{0out} \\ A_{2,T+1}^{Cout} = A_2^{0out} + (1-h)\theta_2 A_{1,T}^{Cout} + (1-h)\theta_2 A_{5,T}^{Cout} \\ A_{3,T+1}^{Cout} = A_3^{0out} + (1-h)\theta_3 A_{2,T}^{Cout} \\ A_{4,T+1}^{Cout} = A_4^{0out} + (1-h)\theta_4 A_{3,T}^{Cout} \\ A_{5,T+1}^{Cout} = A_5^{0out} + (1-h)\theta_5 A_{4,T}^{Cout} \end{cases} \quad (54)$$

We obtain

$$\begin{pmatrix} A_{1,T+1}^{Cout} \\ A_{2,T+1}^{Cout} \\ A_{3,T+1}^{Cout} \\ A_{4,T+1}^{Cout} \\ A_{5,T+1}^{Cout} \end{pmatrix} = \{I + [(1-h)M_b]^1 + [(1-h)M_b]^2 + \dots + [(1-h)M_b]^T\} \begin{pmatrix} A_1^{0out} \\ A_2^{0out} \\ A_3^{0out} \\ A_4^{0out} \\ A_5^{0out} \end{pmatrix}, \quad (55)$$

with

$$M_b = \begin{bmatrix} 0 & 0 & 0 & 0 & 0 \\ \theta_2 & 0 & 0 & 0 & \theta_2 \\ 0 & \theta_3 & 0 & 0 & 0 \\ 0 & 0 & \theta_4 & 0 & 0 \\ 0 & 0 & 0 & \theta_5 & 0 \end{bmatrix}.$$

In the third case, with the the closed cycle of length 5 (Figure 3 (c)), the dynamics of  $\{A_{i,T}^{Cout}\}_{i=1}^5$  is governed by the following system

$$\begin{cases} A_{1,T+1}^{Cout} = A_1^{0out} + (1-h)\theta_1 A_{5,T}^{Cout} \\ A_{2,T+1}^{Cout} = A_2^{0out} + (1-h)\theta_2 A_{1,T}^{Cout} \\ A_{3,T+1}^{Cout} = A_3^{0out} + (1-h)\theta_3 A_{2,T}^{Cout} \\ A_{4,T+1}^{Cout} = A_4^{0out} + (1-h)\theta_4 A_{3,T}^{Cout} \\ A_{5,T+1}^{Cout} = A_5^{0out} + (1-h)\theta_5 A_{4,T}^{Cout} \end{cases} \quad (56)$$

We obtain

$$\begin{pmatrix} A_{1,T+1}^{Cout} \\ A_{2,T+1}^{Cout} \\ A_{3,T+1}^{Cout} \\ A_{4,T+1}^{Cout} \\ A_{5,T+1}^{Cout} \end{pmatrix} = \{I + [(1-h)M_c]^1 + [(1-h)M_c]^2 + \dots + [(1-h)M_c]^T\} \begin{pmatrix} A_1^{0out} \\ A_2^{0out} \\ A_3^{0out} \\ A_4^{0out} \\ A_5^{0out} \end{pmatrix}, \quad (57)$$

with

$$M_c = \begin{bmatrix} 0 & 0 & 0 & 0 & \theta_1 \\ \theta_2 & 0 & 0 & 0 & 0 \\ 0 & \theta_3 & 0 & 0 & 0 \\ 0 & 0 & \theta_4 & 0 & 0 \\ 0 & 0 & 0 & \theta_5 & 0 \end{bmatrix}.$$

It can be easily shown that given  $\{\theta_i\}_i = \theta$  ( $\forall i$ ) (i.e. under the condition of homogeneous hoarding), all panels  $\alpha = a, b, c$  in Figure (3) create the same amount of  $S_{\alpha,t}^{out} = \sum_{i=1}^{i=5} A_{i,t}^{Cout}$  for all  $t \geq 1$ . This is because in all cases of  $\alpha$  we have the same dynamics  $S_{\alpha,t+1}^{out} = S_{\alpha,1}^{out} + (1-h)\theta S_{\alpha,t}^{out}$  and they also all have the same initial aggregate amount of outgoing collateral, i.e.  $S_{\alpha,1}^{out} = \theta \sum_{i=1}^{i=5} A_i^0$ . In addition, in all panels of Figure (3) we have that  $\lim_{t \rightarrow \infty} S_{\alpha,t}^{out} = \sum_{i=1}^{i=5} \frac{A_i^{0out}}{1-(1-h)\theta} = \frac{\theta \sum_{i=1}^{i=5} A_i^0}{1-(1-h)\theta}$ . Thus, at the fixed point solution to  $A^{Cout}$ ,  $m$  is equal to  $\frac{1}{1-(1-h)\theta}$ .

**Proof of proposition 2** In the case represented by Figure 4 (a),  $k_5^{out} = 0 \rightarrow \delta_5 = 0$ , therefore

$$\begin{cases} A_{1,t=1}^{Cout} = A_1^{0out} = \theta_1 A_1^0 \\ A_{2,t=1}^{Cout} = A_2^{0out} = \theta_2 A_2^0 \\ A_{3,t=1}^{Cout} = A_3^{0out} = \theta_3 A_3^0 \\ A_{4,t=1}^{Cout} = A_4^{0out} = \theta_4 A_4^0 \\ A_{5,t=1}^{Cout} = A_5^{0out} = 0 \end{cases} \quad (58)$$

The dynamics of  $\{A_{i,T}^{Cout}\}_{i=1}^5$  will follow

$$\begin{cases} A_{1,T+1}^{Cout} = A_1^{0out} + (1-h)\theta_1 \frac{A_{3,T}^{Cout}}{2} \\ A_{2,T+1}^{Cout} = A_2^{0out} + (1-h)\theta_2 A_{1,T}^{Cout} \\ A_{3,T+1}^{Cout} = A_3^{0out} + (1-h)\theta_3 A_{2,T}^{Cout} \\ A_{4,T+1}^{Cout} = A_4^{0out} + (1-h)\theta_4 \frac{A_{3,T}^{Cout}}{2} \\ A_{5,T+1}^{Cout} = 0 \end{cases} \quad (59)$$

It follows that

$$\begin{pmatrix} A_{1,T+1}^{Cout} \\ A_{2,T+1}^{Cout} \\ A_{3,T+1}^{Cout} \\ A_{4,T+1}^{Cout} \\ A_{5,T+1}^{Cout} \end{pmatrix} = [I + [(1-h)M_a]^1 + [(1-h)M_a]^2 + \dots + [(1-h)M_a]^t] \begin{pmatrix} A_1^{0out} \\ A_2^{0out} \\ A_3^{0out} \\ A_4^{0out} \\ 0 \end{pmatrix}, \quad (60)$$

with

$$M_a = \begin{bmatrix} 0 & 0 & \frac{\theta_1}{2} & 0 & 0 \\ \theta_2 & 0 & 0 & 0 & 0 \\ 0 & \theta_3 & 0 & 0 & 0 \\ 0 & 0 & \frac{\theta_4}{2} & 0 & 0 \\ 0 & 0 & 0 & 0 & 0 \end{bmatrix}.$$

In the case represented by Figure 4 (b), we still have that

$$\begin{cases} A_{1,t=1}^{Cout} = A_1^{0out} = \theta_1 A_1^0 \\ A_{2,t=1}^{Cout} = A_2^{0out} = \theta_2 A_2^0 \\ A_{3,t=1}^{Cout} = A_3^{0out} = \theta_3 A_3^0 \\ A_{4,t=1}^{Cout} = A_4^{0out} = \theta_4 A_4^0 \\ A_{5,t=1}^{Cout} = A_5^{0out} = 0 \end{cases} \quad (61)$$

The dynamics of  $\{A_{i,T}^{Cout}\}_{i=1}^5$  will follow

$$\begin{cases} A_{1,T+1}^{Cout} = A_1^{0out} + (1-h)\theta_1 \frac{A_{4,T}^{Cout}}{2} \\ A_{2,T+1}^{Cout} = A_2^{0out} + (1-h)\theta_2 A_{1,T}^{Cout} \\ A_{3,T+1}^{Cout} = A_3^{0out} + (1-h)\theta_3 A_{2,T}^{Cout} \\ A_{4,T+1}^{Cout} = A_4^{0out} + (1-h)\theta_4 A_{3,T}^{Cout} \\ A_{5,T+1}^{Cout} = 0 \end{cases} \quad (62)$$

We obtain

$$\begin{pmatrix} A_{1,T+1}^{Cout} \\ A_{2,T+1}^{Cout} \\ A_{3,T+1}^{Cout} \\ A_{4,T+1}^{Cout} \\ A_{5,T+1}^{Cout} \end{pmatrix} = [I + [(1-h)M_b]^1 + [(1-h)M_b]^2 + \dots + [(1-h)M_b]^t] \begin{pmatrix} A_1^{0out} \\ A_2^{0out} \\ A_3^{0out} \\ A_4^{0out} \\ 0 \end{pmatrix}, \quad (63)$$

with

$$M_b = \begin{bmatrix} 0 & 0 & 0 & \frac{\theta_1}{2} & 0 \\ \theta_2 & 0 & 0 & 0 & 0 \\ 0 & \theta_3 & 0 & 0 & 0 \\ 0 & 0 & \theta_4 & 0 & 0 \\ 0 & 0 & 0 & 0 & 0 \end{bmatrix}.$$

Furthermore, in the case represented by Figure 4 (c), as shown in (51) and (57), we have

$$\begin{cases} A_{1,t=1}^{Cout} = A_1^{0out} = \theta_1 A_1^0 \\ A_{2,t=1}^{Cout} = A_2^{0out} = \theta_2 A_2^0 \\ A_{3,t=1}^{Cout} = A_3^{0out} = \theta_3 A_3^0 \\ A_{2,t=1}^{Cout} = A_4^{0out} = \theta_4 A_4^0 \\ A_{3,t=1}^{Cout} = A_5^{0out} = \theta_5 A_5^0 \end{cases}$$

Thus

$$\begin{pmatrix} A_{1,T+1}^{Cout} \\ A_{2,T+1}^{Cout} \\ A_{3,T+1}^{Cout} \\ A_{4,T+1}^{Cout} \\ A_{5,T+1}^{Cout} \end{pmatrix} = \{I + [(1-h)M_c]^1 + [(1-h)M_c]^2 + \dots + [(1-h)M_c]^T\} \begin{pmatrix} A_1^{0out} \\ A_2^{0out} \\ A_3^{0out} \\ A_4^{0out} \\ A_5^{0out} \end{pmatrix},$$

with

$$M_c = \begin{bmatrix} 0 & 0 & 0 & 0 & \theta_1 \\ \theta_2 & 0 & 0 & 0 & 0 \\ 0 & \theta_3 & 0 & 0 & 0 \\ 0 & 0 & \theta_4 & 0 & 0 \\ 0 & 0 & 0 & \theta_5 & 0 \end{bmatrix}.$$

We can see that the main difference between Figure 4 (a) and Figure 4 (b) is mathematically expressed by the difference between  $M_a$  and  $M_b$ : in the **latter** case, a part of the initial outgoing collateral from bank 4 is flowing into the cycle, while in the **former** case all outgoing collateral from bank 4 gets stuck in the box of bank 5 and can not be re-used. In addition, comparing these cases to the one represented by Figure 4 (c), we can see that in Figure 4 (c) the initial outgoing collateral from each bank can be re-used infinitely. Defining  $S_{a,t}^{out}$ ,  $S_{b,t}^{out}$ , and  $S_{c,t}^{out}$  are respectively the total amount of outgoing collateral of all banks in Figures 4 (a), (b), and (c) after  $t$  times of using and re-using collateral, it can be proved by induction that  $S_{a,t}^{out} < S_{b,t}^{out} < S_{c,t}^{out}$  ( $\forall t \geq 2$ ). This implies that in contrast to the example illustrated in Figure (3), now longer cycles will generate more collateral.

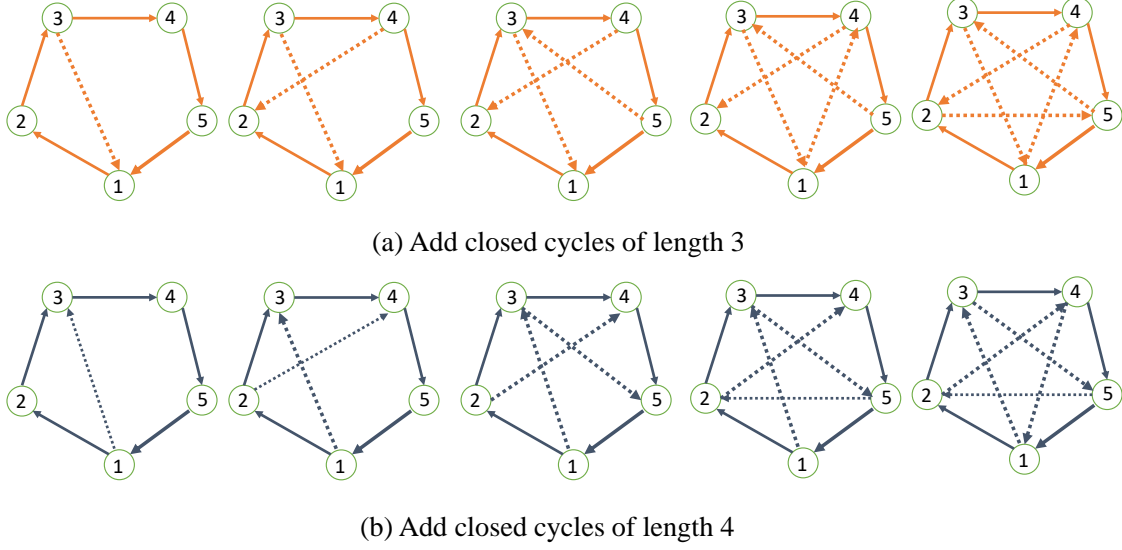


Figure 10: Add different cycles (with length  $k = 3, \dots, N - 1$ ) to an initial closed graph of size  $N$ . An example is illustrated with  $N = 5$  nodes. In the panel (a), we add cycles of length 3. In the panel (b), we add cycles of length 4.

**Proof for proposition 3.**

First, since  $k_i^{out} > 0$ , hence  $\delta_i = 1$  ( $\forall i$ ). Accordingly, we have  $A_i^{C^{out}} = \theta A_i^C$  and  $A_i^{0^{out}} = \theta A_i^0$ . Therefore,

$$S^{out} = \sum_{i=1}^{i=N} A_i^{C^{out}} = \theta \sum_{i=1}^{i=N} A_i^C \quad (64)$$

and

$$m = \frac{\sum_{i=1}^{i=N} A_i^{C^{out}}}{\sum_{i=1}^{i=N} A_i^{0^{out}}} = \frac{\theta \sum_{i=1}^{i=N} A_i^C}{\theta \sum_{i=1}^{i=N} A_i^0} = \frac{\sum_{i=1}^{i=N} A_i^C}{\sum_{i=1}^{i=N} A_i^0}. \quad (65)$$

In addition, since each column<sup>26</sup> of the matrix of shares  $\mathcal{S} = \{s_{i \leftarrow j}\}_{N \times N}$  is summing to 1 and thus  $(1 - h) \sum_{i \neq j} w_{i \leftarrow j} = (1 - h)\theta$ , ( $\forall j$ ), at the fixed point solution to  $A^C$ , we always have

$$\sum_{i=1}^{i=N} A_i^C = (1 - h)\theta \sum_{i=1}^{i=N} A_i^C + \sum_{i=1}^{i=N} A_i^0.$$

Equivalently,

$$\frac{\sum_{i=1}^{i=N} A_i^C}{\sum_{i=1}^{i=N} A_i^0} = \frac{1}{1 - (1 - h)\theta}.$$

Hence, from equations (64) and (67) we have

$$S^{out} = \theta \sum_{i=1}^{i=N} A_i^C = \frac{\theta}{1 - (1 - h)\theta} \sum_{i=1}^{i=N} A_i^0 \quad (66)$$

<sup>26</sup>Now all columns are non-zero since  $k_i^{out} > 0$  for all  $i$ .

and

$$m = \frac{\sum_{i=1}^{i=N} A_i^{C^{out}}}{\sum_{i=1}^{i=N} A_i^{0^{out}}} = \frac{1}{1 - (1-h)\theta}. \quad (67)$$

Notice that when  $A_i^0 = A^0(\forall i)$ , equation (66) leads to

$$S^{out} = \frac{\theta}{1 - (1-h)\theta} N A^0. \quad (68)$$

#### Proof for proposition 4.

To illustrate this proposition, without loss of generality we show an example of closed cycle of length  $N = 5$  in Figure (10). We can add arbitrary links or cycles of length  $k = 3, 4$  to the initial graph. In all examples shown in Figure (10), we always have that  $k_i^{out} > 0$  for every bank  $i$ . Proposition (4) is therefore just a special case of Proposition (3).

#### Proof of proposition 6.

Recall that under the basic model with homogeneous  $\theta$  we have

$$A_i^C = A_i^0 + (1-h)\theta \sum_{j \in B_i} s_{i \leftarrow j} \delta_j A_j^C,$$

where

$$\begin{cases} \delta_j = 1, & \text{if } k_j^{out} > 0 \\ \delta_j = 0, & \text{if } k_j^{out} = 0 \end{cases}$$

Therefore,

$$\mathbb{E}[A_i^C] = A_i^0 + (1-h)\theta \mathbb{E}\left[\sum_{j \in B_i} s_{i \leftarrow j} \delta_j A_j^C\right], \quad (69)$$

where the notation  $\mathbb{E}[X]$  stands for the expectation of  $X$ . With the shares  $s_{i \leftarrow j}$  defined as in equation (1) in the main text, we have

$$\mathbb{E}[A_i^C] = A_i^0 + (1-h)\theta \sum_{j \in B_i} P(k_j^{out} > 0) \mathbb{E}\left[\frac{a_{i \leftarrow j}}{k_j^{out}} A_j^C\right], \quad (70)$$

where  $P(k_j^{out} > 0)$  is the probability that  $k_j^{out} > 0$  and  $P(k_j^{out} = 0)$  is the probability that  $k_j^{out} = 0$ .

Under random graphs with a probability  $p$  of a link between any two nodes (i.e.  $P(a_{i \leftarrow j} = 1) = p$ ), for every  $j$  it is easy to show that  $P(k_j^{out} = 0) = P(k_j^{in} = 0) = (1-p)^{(N-1)}$  and  $P(k_j^{out} > 0) = P(k_j^{in} > 0) = 1 - (1-p)^{(N-1)}$ . In addition,  $\mathbb{E}[k_j^{out}] = \mathbb{E}[k_j^{in}] = p(N-1)$ . That leads to

$$\mathbb{E}[A_i^C] = A_i^0 + [1 - (1-p)^{(N-1)}](1-h)\theta \sum_{j \neq i} \mathbb{E}[P(a_{i \leftarrow j} = 1) \frac{a_{i \leftarrow j}}{k_j^{out}} A_j^C]. \quad (71)$$

From equation (71) we have<sup>27</sup>

$$\mathbb{E}[A_i^C] \approx A_i^0 + [1 - (1-p)^{(N-1)}](1-h)\theta \frac{1}{N-1} \sum_{j \neq i} \mathbb{E}[A_j^C] \quad (72)$$

and the following approximation<sup>28</sup>

$$\mathbb{E}\left[\sum_{i=1}^N A_i^C\right] \approx \frac{\sum_{i=1}^N A_i^0}{1 - [1 - (1-p)^{(N-1)}](1-h)\theta}. \quad (73)$$

<sup>27</sup>We use the approximation  $\mathbb{E}[XY] \approx \mathbb{E}[X] \mathbb{E}[Y]$ .

<sup>28</sup>We use the approximation  $\mathbb{E}\left[\frac{X}{Y}\right] \approx \frac{\mathbb{E}[X]}{\mathbb{E}[Y]}$ .

Thus,

$$\lim_{p \rightarrow 1} \frac{\mathbb{E}[\sum_{i=1}^N A_i^C]}{\sum_{i=1}^N A_i^0} = \frac{1}{1 - (1-h)\theta}. \quad (74)$$

Note that

$$\begin{cases} \mathbb{E}[A_i^{C^{out}}] = P(k_i^{out} > 0)\theta \mathbb{E}[A_i^C] = (1 - (1-p)^{(N-1)})\theta \mathbb{E}[A_i^C] \\ \mathbb{E}[A_i^{0^{out}}] = P(k_i^{out} > 0)\theta A_i^0 = (1 - (1-p)^{(N-1)})\theta A_i^0 \end{cases} \quad (75)$$

Consequently,

$$\mathbb{E}[\sum_{i=1}^N A_i^{0^{out}}] = [1 - (1-p)^{(N-1)}]\theta \sum_{i=1}^N A_i^0 \quad (76)$$

and

$$\mathbb{E}[\sum_{i=1}^N A_i^{C^{out}}] \approx \frac{[1 - (1-p)^{(N-1)}]\theta \sum_{i=1}^N A_i^0}{1 - [1 - (1-p)^{(N-1)}](1-h)\theta}. \quad (77)$$

Hence,

$$\mathbb{E}[m] \approx \frac{\mathbb{E}[\sum_{i=1}^N A_i^{C^{out}}]}{\mathbb{E}[\sum_{i=1}^N A_i^{0^{out}}]} = \frac{1}{1 - [1 - (1-p)^{(N-1)}](1-h)\theta} \quad (78)$$

and

$$\lim_{p \rightarrow 1} \frac{\mathbb{E}[\sum_{i=1}^N A_i^{C^{out}}]}{\mathbb{E}[\sum_{i=1}^N A_i^{0^{out}}]} = \lim_{p \rightarrow 1} \frac{1}{1 - [1 - (1-p)^{(N-1)}](1-h)\theta} = \frac{1}{1 - (1-h)\theta}. \quad (79)$$

Moreover, we can easily show that the approximations for  $\mathbb{E}[\sum_{i=1}^N A_i^C]$ ,  $\mathbb{E}[\sum_{i=1}^N A_i^{0^{out}}]$ , and  $\mathbb{E}[m]$  are increasing functions of the network density  $p$ . In addition, given  $p$  in  $(0, 1]$ , these measures are also increasing functions of the size of the network,  $N$ .

We now proceed with proving the second part of the proposition. We consider a core-periphery graphs in which: (i) the number of nodes in the core,  $N_{core}$ , is fixed; (ii) each node in the periphery has only out-going links, and all point to nodes in the core; (iii) each node in the core are also randomly connected to each other with probability  $p_{core}$ , and there are no directed links from the core to the periphery nodes.

To begin, we first consider the behavior of nodes in the periphery part (Per). For every node  $j$  in the periphery, we have

$$\begin{cases} k_j^{out} \geq 1 \\ \delta_j = 1 \end{cases}$$

and

$$\begin{cases} A_j^{C^{out}} = A_j^{0^{out}} = \theta A_j^0 \\ A_j^C = A_j^0 \end{cases}$$

Therefore,

$$\sum_{j \in \text{Per}} A_j^{C^{out}} = \theta \sum_{j \in \text{Per}} A_j^0, \quad (80)$$

and

$$\sum_{j \in \text{Per}} A_j^C = \sum_{j \in \text{Per}} A_j^0. \quad (81)$$

Equations (80) and (81) imply that the aggregate amounts of in-flowing and out-going collateral of all nodes in the periphery remain constant during rehypothecation process. This observation is intuitive since we assume that periphery banks are purely borrowers and therefore they do not receive collateral from other banks.

Moving on to the core part, for every bank  $i$  in the core part (Core) we have

$$A_i^C = A_i^0 + (1-h)\theta \sum_{j \in \text{Per}} s_{i \leftarrow j} \delta_j A_j^C + (1-h)\theta \sum_{j \in \text{Core}} s_{i \leftarrow j} \delta_j A_j^C. \quad (82)$$

Taking the expectation from both sides, we have

$$\mathbb{E}[A_i^C] = A_i^0 + (1-h)\theta \sum_{j \in \text{Per}} s_{i \leftarrow j} A_j^0 + (1-h)\theta \mathbb{E} \left[ \sum_{j \in \text{Core}} s_{i \leftarrow j} \delta_j A_j^C \right], \quad (83)$$

Defining

$$\tilde{A}_i^0 = A_i^0 + (1-h)\theta \sum_{j \in \text{Per}} s_{i \leftarrow j} A_j^0, \quad (84)$$

then we have

$$\mathbb{E}[A_i^C] = \tilde{A}_i^0 + (1-h)\theta \mathbb{E} \left[ \sum_{j \in \text{Core}} s_{i \leftarrow j} \delta_j A_j^C \right]. \quad (85)$$

Equations (84) and (82) respectively imply two important characteristics of the rehypothecation of collateral under the considered core-periphery structure, i.e. the concentration into the core part and the reuse of collateral among banks in the core.

In addition, since each non-zero column of the matrix of shares  $\mathcal{S} = \{s_{i \leftarrow j}\}_{N \times N}$  is summing to 1, it is easy to show that

$$\sum_{i \in \text{Core}} \tilde{A}_i^0 = \sum_{i \in \text{Core}} A_i^0 + (1-h)\theta \sum_{j \in \text{Per}} A_j^0. \quad (86)$$

Since nodes in the core are assumed to be randomly connected with the density  $p_{\text{core}}$ , using the results obtained from random graphs we have

$$\mathbb{E} \left[ \sum_{i \in \text{Core}} A_i^C \right] = \frac{\sum_{i \in \text{Core}} \tilde{A}_i^0}{1 - [1 - (1-p)^{(N_{\text{core}}-1)}](1-h)\theta}. \quad (87)$$

Equations (81) and (87) lead to

$$\mathbb{E} \left[ \sum_{i=1}^N A_i^C \right] = \mathbb{E} \left[ \sum_{i \in \text{Per}} A_i^C \right] + \mathbb{E} \left[ \sum_{i \in \text{Core}} A_i^C \right] = \sum_{i \in \text{Per}} A_j^0 + \frac{\sum_{i \in \text{Core}} \tilde{A}_i^0}{1 - [1 - (1-p_{\text{core}})^{(N_{\text{core}}-1)}](1-h)\theta}. \quad (88)$$

Note that, for every node  $i$  in the core part

$$\begin{cases} \mathbb{E}[A_i^{C^{out}}] = P(k_i^{out} > 0) \theta \mathbb{E}[A_i^C] = [1 - (1-p_{\text{core}})^{(N_{\text{core}}-1)}] \theta \mathbb{E}[A_i^C] \\ \mathbb{E}[A_i^{0^{out}}] = P(k_i^{out} > 0) \theta A_i^0 = [1 - (1-p_{\text{core}})^{(N_{\text{core}}-1)}] \theta A_i^0 \end{cases} \quad (89)$$

Therefore,

$$\mathbb{E} \left[ \sum_{i \in \text{Core}} A_i^{C^{out}} \right] = \frac{[1 - (1-p_{\text{core}})^{(N_{\text{core}}-1)}] \theta \sum_{i \in \text{Core}} \tilde{A}_i^0}{1 - [1 - (1-p_{\text{core}})^{(N_{\text{core}}-1)}](1-h)\theta}, \quad (90)$$

and

$$\mathbb{E} \left[ \sum_{i \in \text{Core}} A_i^{0^{out}} \right] = [1 - (1-p_{\text{core}})^{(N_{\text{core}}-1)}] \theta \sum_{i \in \text{Core}} A_i^0. \quad (91)$$

From (80) and (90) we have

$$\mathbb{E} \left[ \sum_{i=1}^N A_i^{C^{out}} \right] = \mathbb{E} \left[ \sum_{j \in \text{Per}} A_j^{C^{out}} \right] + \mathbb{E} \left[ \sum_{i \in \text{Core}} A_i^{C^{out}} \right] = \theta \sum_{j \in \text{Per}} A_j^0 + \frac{[1 - (1-p_{\text{core}})^{(N_{\text{core}}-1)}] \theta \sum_{i \in \text{Core}} \tilde{A}_i^0}{1 - [1 - (1-p_{\text{core}})^{(N_{\text{core}}-1)}](1-h)\theta}, \quad (92)$$

which can be simplified as

$$\mathbb{E} \left[ \sum_{i=1}^N A_i^{C^{out}} \right] = \frac{\theta \sum_{j \in \text{Per}} A_j^0 + [1 - (1-p_{\text{core}})^{(N_{\text{core}}-1)}] \theta \sum_{i \in \text{Core}} A_i^0}{1 - [1 - (1-p_{\text{core}})^{(N_{\text{core}}-1)}](1-h)\theta} \quad (93)$$

by substituting  $\tilde{A}_i^0$  in equation (86) into equation (92).

Moreover, the expectation of the aggregate amount of initial out-going collateral is

$$\mathbb{E}[\sum_{i=1}^N A_i^{0out}] = \mathbb{E}[\sum_{j \in \text{Per}} A_j^{0out}] + \mathbb{E}[\sum_{i \in \text{Core}} A_i^{0out}] = \theta \sum_{j \in \text{Per}} A_j^0 + [1 - (1 - p_{core})^{(N_{core}-1)}] \theta \sum_{i \in \text{Core}} A_i^0. \quad (94)$$

As results,

$$\mathbb{E}[m] \approx \frac{\mathbb{E}[\sum_{i=1}^N A_i^{Cout}]}{\mathbb{E}[\sum_{i=1}^N A_i^{0out}]} = \frac{1}{1 - [1 - (1 - p_{core})^{(N_{core}-1)}](1 - h)\theta}, \quad (95)$$

and

$$\lim_{p_{core} \rightarrow 1} \frac{\mathbb{E}[\sum_{i=1}^N A_i^{Cout}]}{\mathbb{E}[\sum_{i=1}^N A_i^{0out}]} = \frac{1}{1 - (1 - h)\theta}. \quad (96)$$

Again, it can be shown that  $\mathbb{E}[\sum_{i=1}^N A_i^C]$ ,  $\mathbb{E}[\sum_{i=1}^N A_i^{0out}]$  and the approximation for  $\mathbb{E}[m]$  are increasing functions of the density of the core  $p_{core}$ . In addition, these three measures are also increasing functions of the size of the core part,  $N_{core}$ , given  $p_{core}$  in  $(0, 1]$ . Comparing the multiplier estimated for core-periphery graphs, (95) and with the one estimated for random graphs (78), we notice that the former is always larger than the latter, as long as  $p_{core} > 1 - (1 - p)^{\frac{N-1}{N_{core}-1}} = p_{th}$ , thus verifying the third part of the proposition. Finally, by inspecting equations (79) and (96) we verify the fourth and final part of the proposition.

#### Proof for proposition 7.

We will now provide detailed derivations for the equilibrium existence to non-hoarded parameters determined under the Value-at-Risk strategy. To begin, let us start with the following definitions:

*Definition 1.* For each column vector  $X = [X_1, X_2, \dots, X_{N-1}, X_N]^T \in \mathbb{R}_+^N$ ,  $X \geq \frac{1}{(1-h)} C^0$  (where  $C^0 = [c_1^0, c_2^0, \dots, c_{N-1}^0, c_N^0]^T$ ), the elements of the matrix  $\tilde{W}^{\text{VaR}}(X)$  (size  $N \times N$ ) is defined as

$$\begin{cases} \tilde{W}_{i \leftarrow j}^{\text{VaR}} = \frac{(1-h)X_j - c_j^0}{X_j k_j^{\text{out}}}, \forall i \in L_j \neq \emptyset, \\ \tilde{W}_{i \leftarrow j}^{\text{VaR}} = 0, \text{ elsewhere.} \end{cases} \quad (97)$$

We will show that the following system of equations

$$X = A^0 + \tilde{W}^{\text{VaR}}(X)X \quad (98)$$

has a single unique solution if  $0 \leq h < 1$  and  $\tilde{\mathcal{A}}^{-1}\tilde{b} \geq \frac{c^0}{1-h}$ , where  $\tilde{b}$  is a column vector size  $N \times 1$ , with

$$\tilde{b} = A^0 - \mathcal{S}C^0 \quad (99)$$

and

$$\tilde{\mathcal{A}} = I - (1-h)\mathcal{S} \quad (100)$$

and the matrix of shares,  $\mathcal{S}$ , is defined as in equation (1) in the main text. Notice that

$$X = A^0 + \tilde{W}^{\text{VaR}}(X)X$$

$\Leftrightarrow$

$$X_i = A_i^0 + \sum_{j \neq i} \frac{a_{i \leftarrow j}}{k_j^{\text{out}}} [(1-h)X_j - c_j^0], \forall i = 1, 2, \dots, N. \quad (101)$$

$\Leftrightarrow$

$$A_i^0 - \sum_{j \neq i} \frac{a_{i \leftarrow j}}{k_j^{\text{out}}} c_j^0 = X_i - \sum_{j \neq i} \frac{(1-h)a_{i \leftarrow j}}{k_j^{\text{out}}} X_j, \forall i = 1, 2, \dots, N. \quad (102)$$

Equivalently,

$$\tilde{b} = \tilde{\mathcal{A}}X \quad (103)$$

If  $\tilde{\mathcal{A}}$  is an invertible matrix, system (103) has a single unique solution

$$X = \tilde{\mathcal{A}}^{-1}\tilde{b}. \quad (104)$$

We now show the invertibility of  $\tilde{\mathcal{A}}$  by reductio ad absurdum. Suppose that  $\tilde{\mathcal{A}}$  is not invertible, then  $\det(\tilde{\mathcal{A}}) = 0$ . Note that  $\tilde{\mathcal{A}} = I - (1 - h)\mathcal{S}$  therefore  $\det(\tilde{\mathcal{A}}) = 0$  if and only if  $\frac{1}{1-h} (> 1)$  is an eigenvalue of  $\mathcal{S}$ . However, since each non-zero column of  $\mathcal{S}$  is summing to 1, according to Perron-Frobenius theorem, the largest eigenvalue of  $\mathcal{S}$  can not be larger than 1.